

JOHNSTON, THOMAS A., M.S., Use of Adsorbent Resins in Fermentations of Bacteria Obtained from the Red Soils of the Kingdom of Jordan and The Isolation and Structure Elucidation of Cytotoxic Xanthenes from an Unidentified Fungus. (2012)

Directed by Dr. Nicholas H. Oberlies, 56 pp.

Part I: Adsorbent resins are used in industrial fermentations to help boost the production of antibiotics. The resins used here were utilized to help speed the drug discovery process by eliminating the time-consuming step of freeze-drying the fermentation extract. This led to a shortened time span from receiving the fermentation to identifying the secondary metabolites via HPLC and LC/MS.

Part II: Three new xanthenes, 1-hydroxy-5-hydroxymethyl-6-methoxy-7-methyl-xanthone (**1**), 1-hydroxy-6-methoxy-7-methyl-xanthone (**2**), and 1-hydroxy-5,7-dimethyl-6-methoxy-xanthone (**3**), were isolated from an unknown fungus, MSX 68425, from the Mycosynthetix library of filamentous fungi. The compounds were discovered using bioactivity-directed fractionation, in pursuit of anticancer lead compounds. The structures of these compounds were determined by spectroscopic and spectrometric techniques, in conjunction with comparisons to the literature.

USE OF ADSORBENT RESINS IN FERMENTATIONS OF BACTERIA OBTAINED
FROM THE RED SOILS OF THE KINGDOM OF JORDAN AND
THE ISOLATION AND STRUCTURE ELUCIDATION OF
CYTOTOXIC XANTHONES FROM AN
UNIDENTIFIED FUNGUS.

by

Thomas A. Johnston

A Thesis Submitted to
the Faculty of the Graduate School at
The University of North Carolina at Greensboro
in Partial Fulfillment
for the Requirements for the Degree
Master of Science

Greensboro
2012

Approved by

Committee Chair

APPROVAL PAGE

This thesis has been approved by the following committee of the Faculty at The University of North Carolina at Greensboro.

Committee Chair _____

Committee Members _____

Date of Acceptance by Committee

Date of Final Oral Examination

ACKNOWLEDGEMENTS

First and foremost, I would like thank my mom and dad, who allowed me to pursue a career path that is my own and who has put up with my antics for so long.

This thesis would not have been possible without the guidance of my research advisor, Dr. Nicholas Oberlies, who aided me through the research and writing process.

I'm grateful to the Oberlies laboratory group for all of the day to day help and motivation. Tyler Graf for helping with instrumentation, Sloan Ayers, Arlene Sy-Cordero, and Mario Figueroa for NMR assistance as well as being great resources to talk to about natural products chemistry. Thank you to the rest of the Oberlies group: Karen VanderMolen, Tamam El-Elimat, Hanan Althagafy, and Huzefa Raja for the support and friendship.

A heartfelt thank you to Franklin Moy for his NMR expertise and Brandie Ehrmann for her expertise in mass spectrometry.

TABLE OF CONTENTS

	Page
LIST OF TABLES	v
LIST OF FIGURES	vi
CHAPTER	
I. INTRODUCTION	1
II. METHODS.....	6
A. Bacterial Fermentations	6
B. XAD Resins.....	6
C. Fermentation Conditions.....	6
D. Extraction.....	7
E. Instrumentation	9
F. Antimicrobial Assay	9
III. RESULTS	10
IV. CONCLUSION.....	17
V. INTRODUCTION	18
VI. METHODS.....	23
A. Fermentation.....	23
B. Instrumentation	23
C. Bioactivity-Directed Fractionation.....	24
D. Purification and Analysis.....	28
E. Human Cancer Cell Panel.....	31
VII. RESULTS	32
A. 01007-150-1 (Compound 1).....	32
B. 01007-150-3 (Compound 2).....	42
C. 01007-150-4 (Compound 3).....	47
D. EC ₅₀	53
VIII. CONCLUSION.....	54
REFERENCES.....	55

LIST OF TABLES

	Page
Table 1. MIC values for extracts of 14-2-1	11
Table 2. Sample ID, bioassay data, and weight obtained for flash chromatography from MSX 68425	27
Table 3. Bioassay data for fractions of 01007-33-2 (renamed 01007-150).....	30
Table 4. NMR data table for compounds (1 – 3	41
Table 5. EC ₅₀ bioassay data	53

LIST OF FIGURES

	Page
Figure 1. Structures of: a) Actinomycin D, b) Actinomycin X2, and c) Actinomycin P2.....	5
Figure 2. Amberlite XAD-7HP acrylic ester matrix.....	8
Figure 3. Three HPLC chromatograms from the three different growth conditions of organism 14-2-1 @245nm: a) Grown with resin for the entire fermentation, b) Grown without resin and resin added for 1 hour at the end of the fermentation, and c) Grown without resin, no resin added at end.....	12
Figure 4. HPLC-MS Chromatogram with UV detection a) Grown with resin for the entire fermentation, b) Grown without resin and resin added for 1 hour at the end of the fermentation, c) Grown without resin, no resin added at end, and d) MeOH blank	14
Figure 5. Mass spectrum: a) 01006-10-1 (RT = 14.5 min) positive mode, b) 01006-10-1 (RT = 15.5 min) positive mode, and c) 01006-10-1 (RT = 16.6 min) positive mode.....	15
Figure 6. Xanthone structural backbone.....	22
Figure 7. Psorospermin, isolated from <i>Psorospermum febrifugum</i>	22
Figure 8. ISCO flash chromatogram of organic extract from organism MSX-68425	26
Figure 9. Analytical HPLC chromatogram of 01007-33-2 @230 nm.....	28
Figure 10. a) Preparative HPLC of 01007-33-2 (vertical black bars represent fractions) and b) pooling based on chromatogram.....	29
Figure 11. Proposed structure of compound 1 (01007-150-1).....	35
Figure 12. UPLC @ 235 nm of compound 1 (01007-150-1) showing >95% purity	35
Figure 13. ¹ H NMR of Compound 1 (CDCl ₃) and expansion of aromatic region (δ _H 6.5-7.0) (inset)	36
Figure 14. ¹³ C NMR data of compound 1	37
Figure 15. COSY NMR data of Compound 1	38

Figure 16. HSQC-edited NMR data of Compound 1	39
Figure 17. HMBC NMR data of Compound 1	40
Figure 18. Proposed structure of 01007-150-3 Compound 2	43
Figure 19. UPLC of Compound 2 @235 nm showing >95% purity	43
Figure 20. ¹ H capNMR of Compound 2 (CDCl ₃) and expansion of aromatic region (δ_{H} 6.5-7.0) (inset).....	44
Figure 21. HSQC-edited spectrum of compound 2 (CDCl ₃ , CapNMR)	45
Figure 22. HMBC spectrum of compound 2 (CDCl ₃ , CapNMR).....	46
Figure 23. Proposed structure of 01007-150-3 Compound 3	48
Figure 24. UPLC of Compound 3 (01007-150-4) showing >95% purity	48
Figure 25. ¹ H NMR data for Compound 3 (CDCl ₃) and expansion of aromatic region (δ_{H} 6.5-8.0) (inset).....	49
Figure 26. ¹³ C NMR of Compound 3 in CDCl ₃ (01007-150-4).....	50
Figure 27. HSQC-edited spectrum of Compound 3 (01007-150-4).....	51
Figure 28. HMBC spectrum of Compound 3 (01007-150-4)	52

CHAPTER I

INTRODUCTION

The discovery and application of Penicillin has widely been hailed as the greatest medical discovery of the 20th century, helping to extend the life expectancy of humans by curing common, and once fatal, infections. The discovery of additional antibiotics also ushered in the overuse of these compounds and modern medicine faces an unfortunate crisis against public health. The rise of antibiotic resistance against some front line antimicrobial compounds is reaching a crisis level and as a result infections that had once become easily treatable, such as staph infection and tuberculosis, are once again public health hazards. This problem has been exacerbated by the falling rate of discovery of novel antimicrobial classes in the laboratory.^{1,2}

The red soils of the Hashemite Kingdom of Jordan have been traditionally used as an anti-infective agent, being utilized to cure skin infections. The traditional method was to create a paste using the soil and topically apply the paste daily onto the site of infection. This traditional use triggered the investigation that determined the antimicrobial properties can be attributed to a host of bacteria, most notably *Actinomycetes* which are known to produce several antimicrobial compounds such as actinomycin.³

Methicillin resistant *Staphylococcus aureus* (MRSA) is a common antibiotic resistant infection due to its prevalence in hospitals and on the human body. The emergence of MRSA as a deadly infection has prompted the more common use of

alternative and more powerful antibiotics, such as vancomycin, that were once reserved only for the most dire of cases due to the potential side effects of the drugs. The use of these “last line” antibiotics has led to the subsequent emergence of resistance against them as well.⁴

Another emerging health hazard is drug resistant tuberculosis (XD-TB) and multiple drug resistant tuberculosis (XDR-TB). This is a major problem in less developed countries with poor sanitation and little public health awareness. Estimates put tuberculosis infections at 2 billion people worldwide with approximately 9 million deaths a year. No new drugs for the treatment of tuberculosis have been commercialized since 1964.⁵

There are several processes of how bacteria can gain antibiotic resistance. Mutation is the most common and well understood. Another process is known as horizontal gene transfer, where a piece of genetic material that allows for resistance is transferred between a species or even across different species.⁶

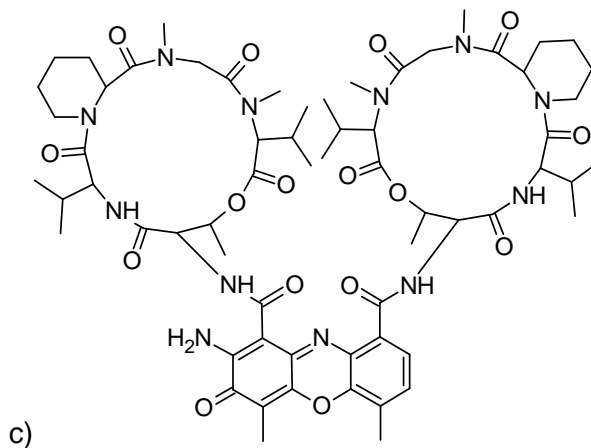
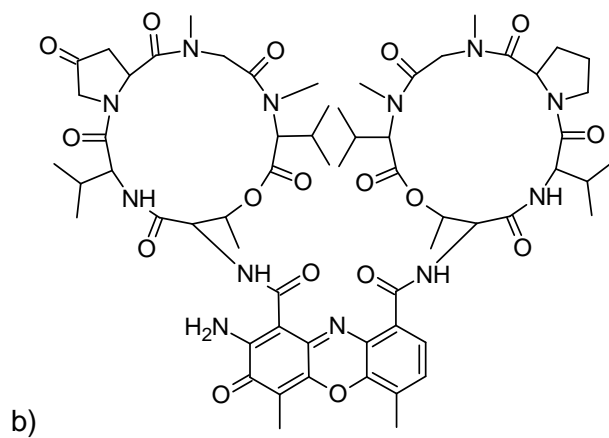
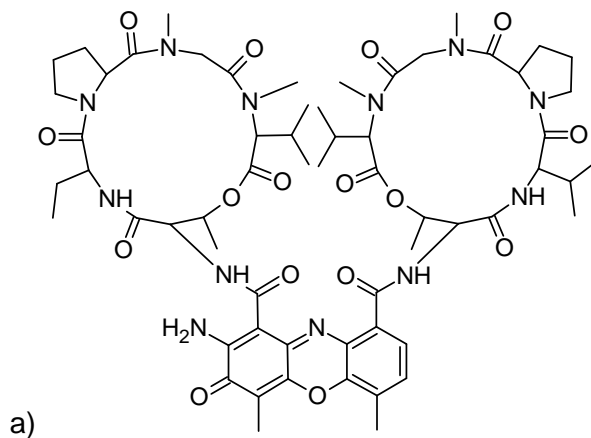
The production of antibiotics is achieved via two routes in the pharmaceutical industry: synthesis and fermentation. Many of the front line antibiotics are synthesized in the laboratory. Many other antibiotics, notably those that are difficult to synthesize, must be fermented by the microorganism that it was discovered in, or a genetically modified version. Teicoplanin is used clinically to treat MRSA and can only be made economically by fermentation.⁷ A problem with this process is yield and extraction from the fermentation. From this, a combination of resins and genetically modified microorganisms are typically used in industrial fermentations of antibiotics to increase yields and ease extraction of the desired product.⁸

The one use of adsorbent resins in fermentations is to prevent the negative feedback inhibition mechanism.⁹ This process is where the production of a certain compound will inhibit its further biosynthesis once a particular concentration has been attained. The resin can also protect the metabolite from enzymatic conversion as the pores on the resin are usually too small for proteins to enter.¹⁰ This allows for an array of different resins to be developed and used for different types of bacterial fermentations. One particular drawback of adsorbent resins is that they are extracellular, and therefore can only interact with metabolites after they have been secreted from the cytoplasm. A goal of the research conducted was to utilize the ability of the resin to adsorb secondary metabolites of the fermentation and subsequently extract the product in the laboratory, eliminating the time consuming steps of freeze drying and flash chromatography of the fermentation extract, thereby hastening the drug discovery process.

The research presented here isolated three analogues of Actinomycin: D, X2, and P2 (order of elution) (figure 1). Actinomycins are polypeptide compounds that exhibit potent antibacterial and anticancer properties. They are produced by the bacterial family *Actinomycete*, most notably from the genus *Streptomyces*. They display potent antimicrobial properties versus Gram positive bacteria, and a weaker activity against Gram negative bacteria and fungi.¹¹ Their mechanism of action (MOA) is to inhibit DNA transcription by preventing the RNA Polymerase from binding and elongating on the DNA strand.¹² Actinomycin D is the form currently used for medicinal purposes in chemotherapy and is generically known as dactinomycin. It has lost its original use as an antibiotic because it can cause genetic damage due to its MOA and the relatively high concentration needed to obtain antibiotic efficacy. Today it is mostly reserved for chemotherapy against Wilm's Tumor (kidney cancer) and Rhabdomyosarcoma (skeletal

muscle cancer). Actinomycin X2 and Actinomycin P2 are not utilized for medicinal purposes.

Figure 1: Structures of: a) Actinomycin D, b) Actinomycin X2, and c) Actinomycin P2



CHAPTER II

METHODS

A. Bacterial Fermentations

The bacterium was identified as a *Streptomyces* sp. from the family *Actinomycetes*. The Bacterium was obtained from the red soils of the Hashemite Kingdom of Jordan. Fermentation was conducted in the laboratory of Dr. Joseph Falkinham III at Virginia Polytechnic University. Fermentations were incubated at 30°C on a shaker for seven days in ¼ strength tryptic soy broth with 2% sucrose (v/v). Bacterial culture purity was checked by streak plate at the end of the fermentation.

B. XAD Resins

The adsorbent resin was Amberlite XAD-7HP (figure 2), an acrylic ester that is moderately hydrophobic. 0.4 g of resin were used in fermentations that required resin. The resin was prewashed before application to the fermentation by a rinse in MeOH for 15 min.

C. Fermentation Conditions

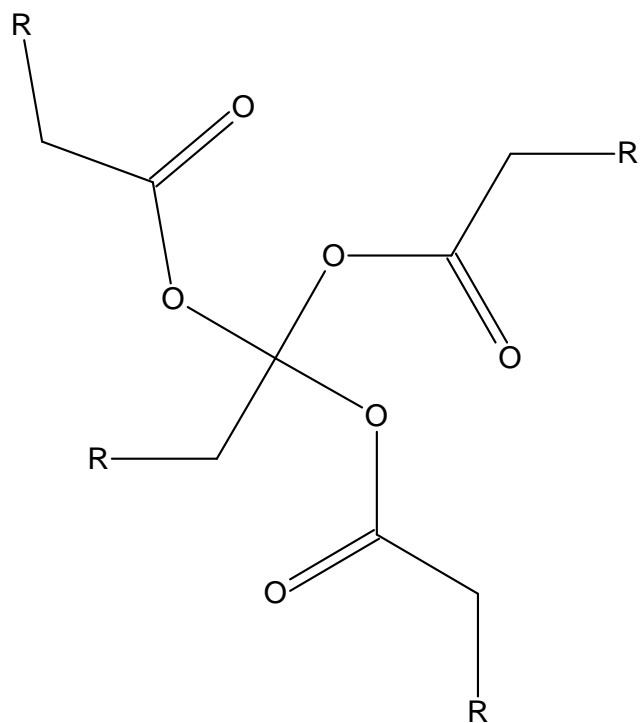
Three fermentation conditions were applied:

- 1) Fermentation proceeded with resin for the entire time.
- 2) Fermentation proceeded without resin; resin was added for 1h at the end.
- 3) Fermentation proceeded without resin.

D. Extraction

The resin was recovered from the fermentation broth by centrifugation and filtration. The resin was stirred in a mixture of 1:1 CHCl_3 :MeOH for several hours to elute adsorbed metabolites from the resin. The resin was filtered out using a vacuum filter system and a Whatman no. 1 filter. Appropriate amounts of CHCl_3 and H_2O were added to obtain a 4:1:5 CHCl_3 :MeOH: H_2O mixture. This mixture was allowed to partition in a separatory funnel, and the lower organic layer was drawn off and evaporated to dryness. An aliquot of the crude extract was tested in an antimicrobial assay (table 1) and the remainder of the fraction was analyzed via RP-HPLC for initial analytical testing. RP-HPLC-MS was utilized to determine the content of the sample. The mass was used as a parameter in the Dictionary of Natural Products database for identification (DNP ver. 20.1).

Figure 2: Amberlite XAD-7HP acrylic ester matrix.



E. Instrumentation

RP-HPLC utilized a YMC ODS-A column (150 x 4.6 mm, 5 μ m) at 1 mL/min with a gradient of 20 to 100% MeOH:H₂O over 25 min. HPLC system was a Varian Prostar equipped with Prostar 210 HPLC pumps and Prostar 335 photodiode array detector. Mass spectrometry analysis was performed on an Agilent 1100 HPLC system with an Agilent Triple-Quadrupole mass spectrometer. The analysis on the RP-HPLC-MS was performed using a Prevail C₁₈ column (50 mm x 2.3 mm, 3 μ m) at 1 mL/min with a gradient of 20 to 100% MeOH over 45 min.

F. Antimicrobial Assay

Micrococcus luteus, *Escherichia coli* and *Saccharomyces cerevisiae* were each grown from a single colony in 0.1-strength brain heart infusion broth (Difco). Cultures were incubated for 18 h at 30°C.¹³ The antimicrobial assay was conducted by broth microdilution in a 96-well plate containing *M. luteus*, *E. coli*, and *S. cerevisiae*. All samples were dissolved in DMSO. Results were reported as the minimum concentration required for the inhibition of all growth of the organism.³

CHAPTER III

RESULTS

Organism 14-2-1 (*Streptomyces* sp.) yielded several secondary metabolites that were extracted from the adsorbent resin and, in case of fermentation condition three, the crude extract. The crude extracts of each fermentation were sent for an antimicrobial assay against three organisms: *Micrococcus luteus* (Gram positive), *Escherichia coli* (Gram negative), and *Saccharomyces cerevisiae* (yeast fungus). The bioassay showed similar results for all three extracts (Table 1).

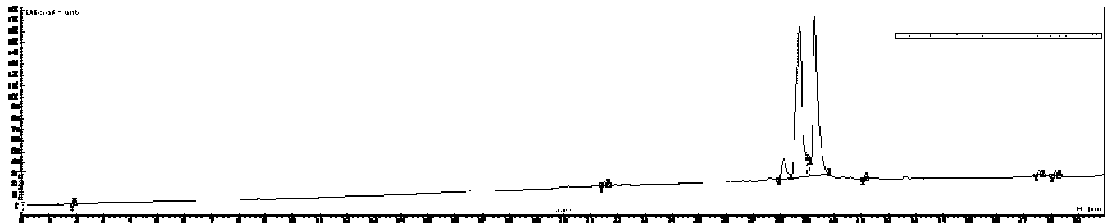
Secondary metabolites were extracted from the resin using the 1:1 CHCl₃:MeOH mixture and partitioned as described above. The lower organic layer was drawn off and dried to attain a starting material weight. This material was analyzed by RP-HPLC to determine the make-up of the sample (Figure 3).

Table 1: MIC values for extracts of 14-2-1. All values reported as $\mu\text{g/mL}$.

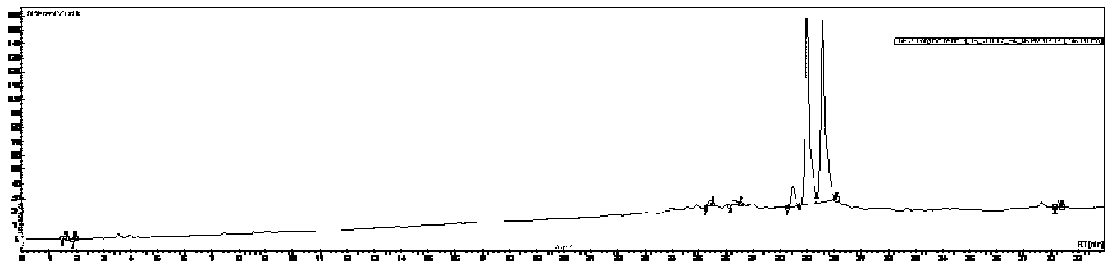
	Grown with resin	Grown without resin, resin added for 1hr.	Grown without resin
<i>Micrococcus luteus</i>	0.3	0.3	0.3
<i>Escherichia coli</i>	110.4	58.3	74.3
<i>Saccharomyces cerevisiae</i>	176.7	181.7	152.1
Fraction weight (mg)	8.4	11.5	13.5

Figure 3: Three HPLC chromatograms from the three different growth conditions of organism 14-2-1 @245nm: a) Grown with resin for the entire fermentation, b) Grown without resin and resin added for 1 hour at the end of the fermentation, and c) Grown without resin, no resin added at end.

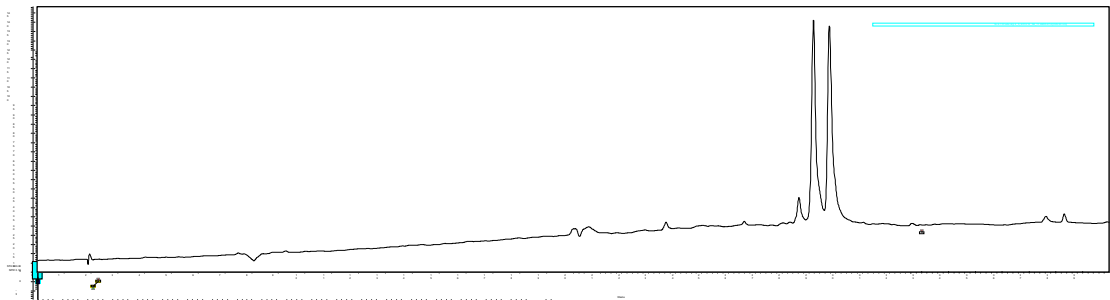
a)



b)



c)



After the gradient was established, the sample was analyzed by RP-HPLC-MS. (figure 4) The first HPLC peak at RT = 14.4 min displayed a $m/z = 1255.27 [M + H]^+$, $m/z = 1277.52 [M + Na]^+$, and $m/z (z = 2) = 628.47 [M + H]^+$. (figure 5a) The second HPLC peak at RT = 15.59 min displayed a $m/z = 1269.42 [M + H]^+$, $m/z = 1291.48 [M + Na]^+$, and $m/z (z = 2) = 635.92 [M + H]^+$. (figure 5b) The third HPLC peak at RT = 15.73 min displayed a $m/z [M + H]^+ = 1283.46$, $m/z [M + Na]^+ = 1305.47$, and $m/z (z = 2) = 635.53 [M + H]^+$.(figure 5c) The $[M + H]^+$ mass data were entered into the Dictionary of Natural Products for reference. The peak at RT = 14.4 min was shown to be Actinomycin D ($m/z = 1254.63 [M + H]^+$) (figure 1a). The peak at RT = 15.59 min was shown to be Actinomycin X2 ($m/z = 1269.45 [M + H]^+$) (figure 1b). The peak at RT = 15.73 min was shown to be Actinomycin P2 ($m/z = 1283.46 [M + H]^+$) (figure 1c). These data are consistent with the taxonomic data on organism 14-2-1, which is an actinomycete and known to produce actinomycins.

Actinomycin D is the version of actinomycin used for comparison of other analogues, yielding a polypeptide sequence of L-Thr, D-Val, L-Pro, Sar, L-MeVal. Actinomycin X2 modifies the 4^{3β} position by oxidizing it to a ketone. Actinomycin P2 modifies the five member ring of the proline amino acid residue by including an extra carbon to make a six member ring. (figure 1)

Figure 4: HPLC-MS Chromatogram with UV detection a) Grown with resin for the entire fermentation, b) Grown without resin and resin added for 1 hour at the end of the fermentation, c) Grown without resin, no resin added at end, and d) MeOH blank

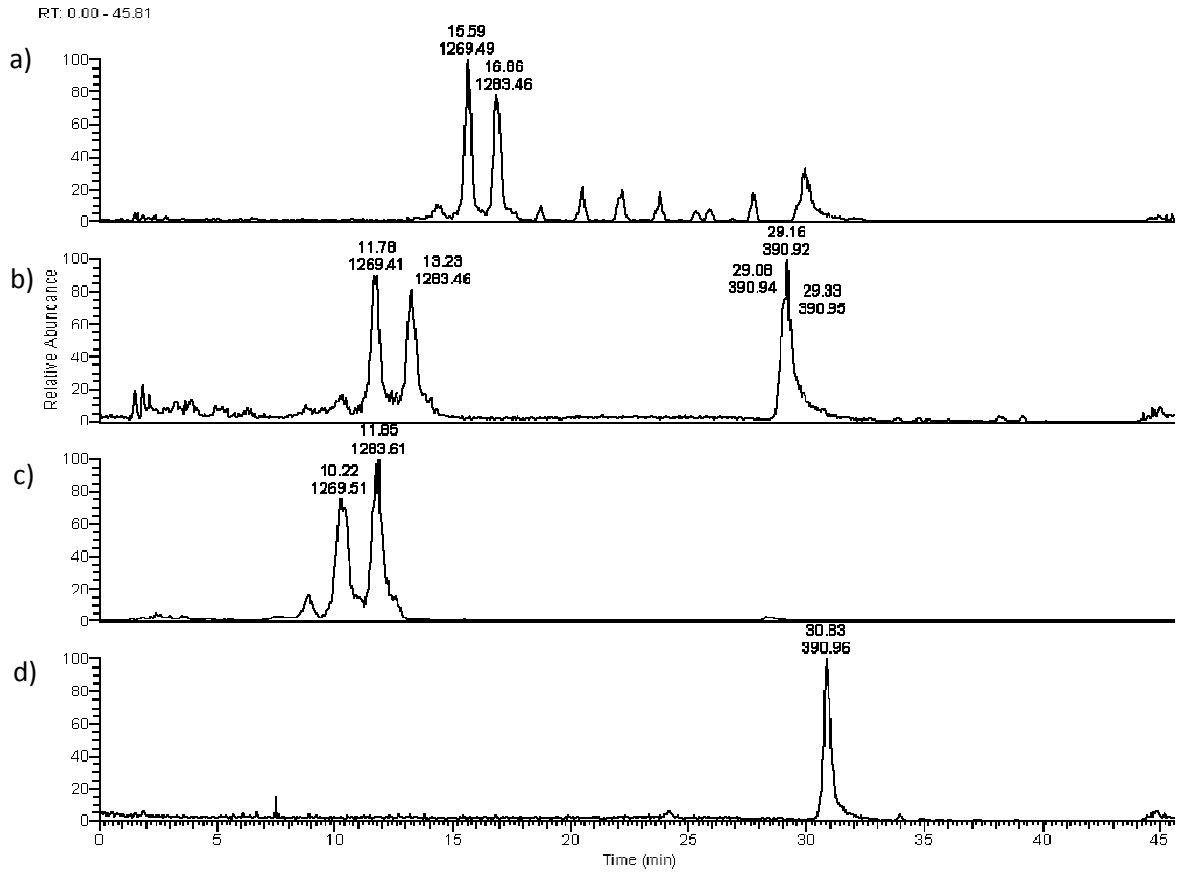
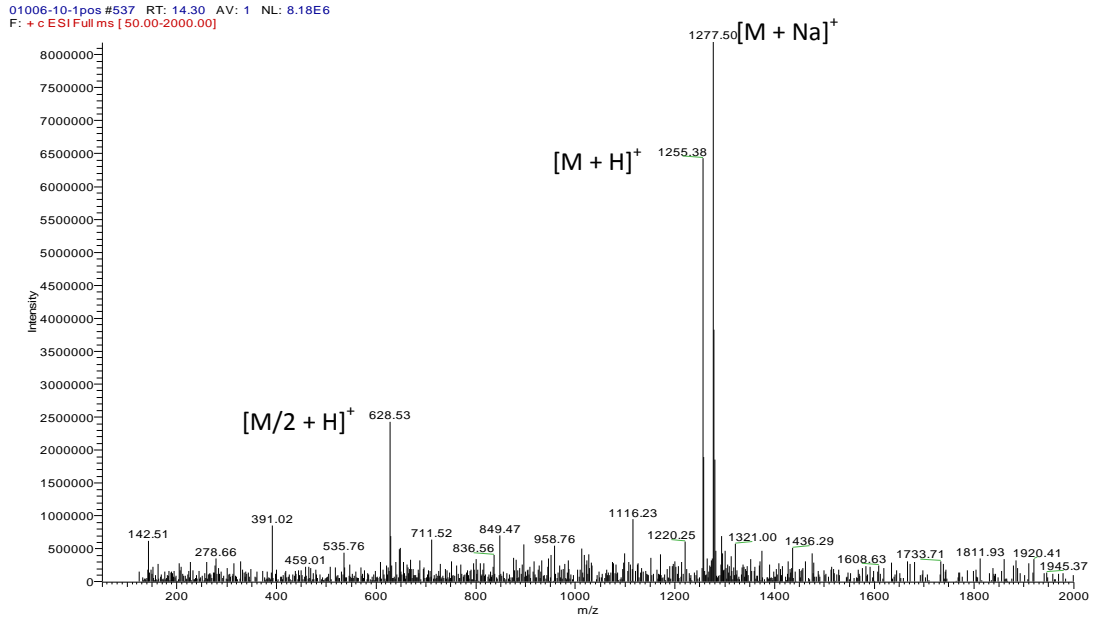
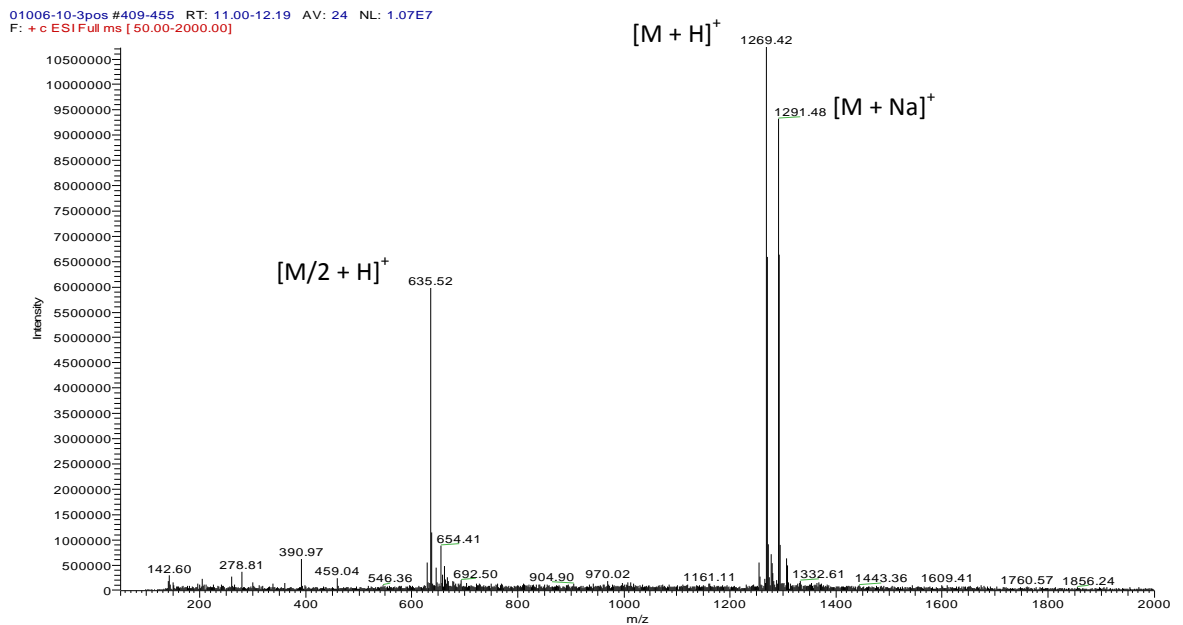


Figure 5: Mass spectrum: a) 01006-10-1 (RT = 14.5 min) positive mode, b) 01006-10-1 (RT = 15.5 min) positive mode, and c) 01006-10-1 (RT = 16.6 min) positive mode

a) Actinomycin D

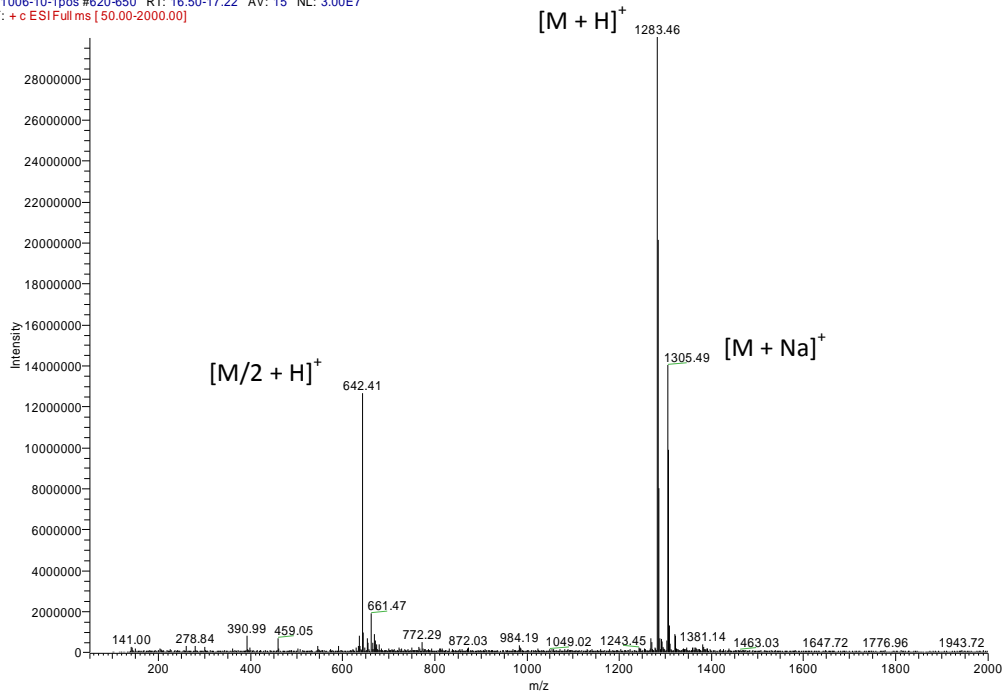


b) Actinomycin X2



c) Actinomycin P2

01006-10-1pos #620-650 RT: 16.50-17.22 AV: 15 NL: 3.00E7
F: + c ESI Full ms [50.00-2000.00]



CHAPTER IV

CONCLUSION

The resin was able to sequester the bioactive compound from the fermentation broth. While there was no apparent boost in production of the product for this particular organism, the recovery of the actinomycin was made easier by the presence of the resin. This eliminated a freeze drying step that was a 24 h process. Some drawbacks to the use of adsorbent resins are the increase in cost of the fermentation.

Extraction of the metabolite from the resin was achieved by using 1:1 CHCl_3 :MeOH mixture. The sequestration of three different forms of actinomycin was also an interesting effect of the experiment. The presence of additional peaks in the LC/MS of the first growth condition allowed for additional study of metabolites that were present in the fermentation broth; these peaks were not present in the chromatograms of the other two growth conditions. The masses of these peaks were entered in the DNP for analysis, and the results were inconclusive.

CHAPTER V

INTRODUCTION

In 2010, 1.5 million new cancers of cancer were reported in the USA, with an estimated 550,000 American deaths being attributed to cancer during the same year.¹⁴ The leading cause of death among females was breast cancer, while males died most from lung cancer in the USA.¹⁵ This has prompted the need for a more diverse array of anticancer agents to be readily available.

The discovery of antimicrobials from natural sources ushered in the discovery of chemotherapeutic agents from natural sources. Vincristine (*Catharanthus roseus*),¹⁶ camptothecin (*Camptotheca acuminata*),¹⁷ and taxol (*Taxus brevifolia* Nutt)¹⁸ were some of the first anticancer agents discovered from plants.¹⁹ Fungi are excellent sources of natural products, and are ubiquitous in nature. The economic impact of fungal natural products is quite enormous, with about 22% of the known 12,000 antimicrobial compounds coming from filamentous fungi combining for a market value of \$4.4 billion dollars.²⁰

The research conducted here focused on the secondary metabolites of filamentous fungi in pursuit of anticancer drug leads. Filamentous fungi are a diverse group within the fungal kingdom, covering most of the higher evolved fungal species (non-yeast) and can be found all over the world. Of course not all of the fungal metabolites are medicinally useful, as fungi also produce mycotoxins, which can cause

serious illness or death. The estimated number of filamentous fungi species is approximated to be 1.5 million, with only around 75,000 (5%) having been described in the literature.²¹

The overall goal of the research was the isolation and structure elucidation of cytotoxic fungal metabolites. The fungus (MSX 68425) was fermented at Mycosynthetix, Inc. in Hillisborough, NC. MSX 68425 was selected for further study based on the bioactivity of the crude extract. A human cancer cell line panel was used to test the crude extract of the organisms for anticancer activity. The three cancer cell lines were:

- MCF-7 human breast carcinoma, a medium growing cell line.²²
- H460 human large cell lung carcinoma, a fast growing cell line.²³
- SF268 human astrocytoma, slow growing cell line.²⁴

A percent survival rate of <20% at an extract concentration of 20 µg/mL is considered an active organism. The overall objective of this cell line panel is to gain entry to the NCI 60 cell line cancer panel with a novel, active anticancer compound.

Dereplication is a method that helps to save time, money, and energy by making the drug discovery process more efficient while being thorough at the same time. This is done by screening out compounds that have already been discovered by comparing UV and High Resolution Mass Spectrometry (HRMS) data in databases. An excellent database is The Dictionary of Natural Products (DNP), which comprises over 200,000 naturally produced compounds in its library. This source allows for the comparison of data from the various analytical techniques to a known library of compounds, such as unique UV spectra, NMR peaks, and the mass of the compound.

The research here yielded three fungal derived xanthenes that displayed moderate cytotoxicity in the human cancer cell panel. All three are new xanthenes, never having been discovered from a natural source before.

A xanthone ($C_{13}H_8O_2$) is a three membered ring system consisting of two benzene rings, one derived from acetate unites (ring A) and one derived from shikimic acid (ring B), joined by a carbonyl and an oxygen to form a central six member ring between the two benzenes that lies flat in the plane, a characteristic of many anticancer drug compounds.²⁵ (figure 6).

Xanthenes are found in many angiosperms (flowering and fruiting plants) as well as fungi and lichens. (Cardona 1990) A search in the Dictionary of Natural Products yielded 900 xanthenes, with ~10% of the 900 assigned xanthenes originating from fungi and the remainder from higher plants.

Xanthenes show a wide spectrum of activity and have been evaluated for anticancer, anti-inflammatory,²⁶ antibiotic,²⁷ antifungal,²⁸ and antioxidant²⁹ properties. The furanoxanthone psorospermin (figure 7), isolated from the plant *Psorospermum febrifugum* Spach, has been identified to have a novel mechanism of action for an antiproliferative agent by being an irreversible DNA topoisomerase II inhibitor. Psorospermin is the target of ongoing DNA alkylation studies, as well as being in preclinical development as anticancer agent.³⁰

Psorospermin has garnered more interest in xanthenes as chemotherapeutic agents, due to its unique interaction with DNA in the cell. Xanthenes interact exclusively with DNA or DNA-protein complexes in the cell, causing DNA breakage or protein binding inhibition, which both lead to cancer cell death. The ability of xanthenes to intercalate

with DNA base pairs, believed to be due to the planar ring system, suggests promise as anticancer drug leads. This has led many scientists to push for discovery of new xanthenes or synthesis of new xanthenes for drug discovery.³¹

Figure 6: Xanthone structural backbone. Ring A is polyketide derived, Ring B is from shikimic acid.

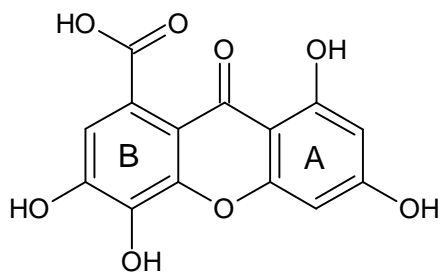
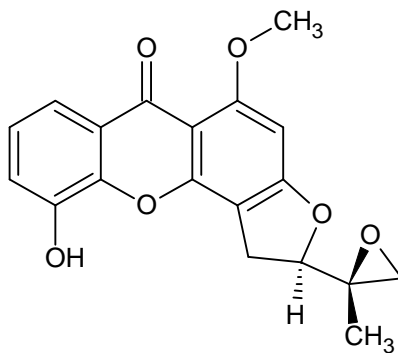


Figure 7: Psorospermin, isolated from *Psorospermum febrifugum*.³¹



CHAPTER VI

METHODS

A. Fermentation

The fungal isolate MSX 68425 was obtained from the Mycosynthetix, Inc. library of filamentous fungi (Hillsborough, NC). Taxonomic studies are ongoing.

The culture was stored on a malt extract slant and transferred periodically. A fresh culture was grown on a similar slant, and a piece was transferred to a medium containing 2% soy peptone, 2% dextrose, and 1% yeast extract (YESD media). Following incubation (7 d) at 22 °C with agitation, the culture was used to inoculate 50 mL of a rice medium, prepared using rice to which was added a vitamin solution and twice the volume of rice with H₂O, in a 250 mL Erlenmeyer flask. This was incubated at 22°C until the culture showed good growth (approximately 14 d).

B. Instrumentation

NMR instrumentation was a JEOL ECA-500, operating at 500 MHz for ¹H and 125 MHz for ¹³C, with JEOL Delta software for analysis. All NMR experiments were in CDCl₃. Compounds **1** and **3** were analyzed using a JEOL 5mm tunable PFG NM-50TH5AT/FG2 probe, while compound **2** was analyzed using a Protasis inverse carbon gradient capillary probe. HRMS was performed on a Thermo-Scientific LTQ-Orbitrap system with an ESI source and Waters Acquity UPLC front end. The operating

parameters for the source were 4.5 kV spray voltage, 1000 V tube lens voltage, a capillary temperature of 270 C, and a sheath gas volume of 15 arb. UPLC conditions were 20:80 → 100% ACN:H₂O over 7 min at 0.6 mL/min on a Prevail C₁₈ column (50 mm x 2.1 mm x 3 μm). HRMS data was collected with Xcalibur software. Normal Phase Flash Chromatography was conducted on a Teledyne-Isco CombiFlash Rf system using a RediSep Rf Si-gel Gold column (Lincoln, NE, USA). HPLC was executed on Varian Prostar HPLC Systems (Walnut Creek, CA, USA) equipped with Prostar 210 HPLC pumps and Prostar 335 photodiode array detector. HPLC data were collected and analyzed with Galaxie Chromatography Workstation Software version 1.9.3.2. Analytical HPLC was performed with a Gemini-NX column (150 x 4.6 mm, 5 μm) at 1 mL/min, preparative HPLC was performed with a Gemini-NX column (250 x 21.2 mm, 5 μm) at 15 mL/min, and semi-preparative HPLC was performed with a Gemini-NX column (250 x 10.0 mm, 5 μm) at 4 mL/min. All three columns were manufactured by Phenomenex (Torrence, CA, USA).

C. Bioactivity-Directed Fractionation

The fungal sample was fermented and a 1:1 CHCl₃:MeOH mixture was added and stirred overnight. The mixture was partitioned in a 4:1:5 CHCl₃:MeOH:H₂O mixture. The organic layer was drawn off and dried to obtain a crude extract. This crude extract was tested in the cancer bioassay for activity. A positive result (<20% survival at 20 μg/mL) in the bioassay of the crude extract points to a further investigation of the organism.

The crude extract was fractionated by an ISCO normal phase flash chromatography system. (Figure 8) This material was fractionated at 40 mL/min on a

RediSep Rf Gold silica gel column (4 g), first with 100% hexanes for 0.7 column volumes (CV) followed by a gradient of 100% hexanes to 100% CHCl₃ over 8.9 CV. The elution continued with 100% CHCl₃ for 7.4 CV, then with a gradient of MeOH in CHCl₃ (0-2% over 9.7 CV, then 2-5% over 5.2 CV, then 5-10% over 5.2 CV, then 10-20% over 3.7 CV, then 20-100% over 2.2 CV. MeOH (100%) was finally held for a further 6.7 CV).

Fractions were collected every 24.75 mL. Five pools were generated by combining fractions, and these were tested for cytotoxicity. Pool 2 (167.4 mg) was cytotoxic and subjected to preparatory RP-HPLC, using a gradient of at 15 mL/min 50-100% CH₃CN in H₂O over 30 min; Elution times and amount isolated were **1**: 11 min (10.2 mg), **2**: 18.5 min (5.8 mg), **3**: 21 min (7.0 mg). Compounds **1** and **3** were >95% pure (via UPLC) after the first round of prep-HPLC, while Compound **2** was 80% pure and required two additional rounds of purification to yield 0.6 mg of pure compound.

Figure 8: ISCO flash chromatogram of organic extract from organism MSX-68425. Blue line is the gradient. Orange line is all wavelength UV. Green line is ELS detection.

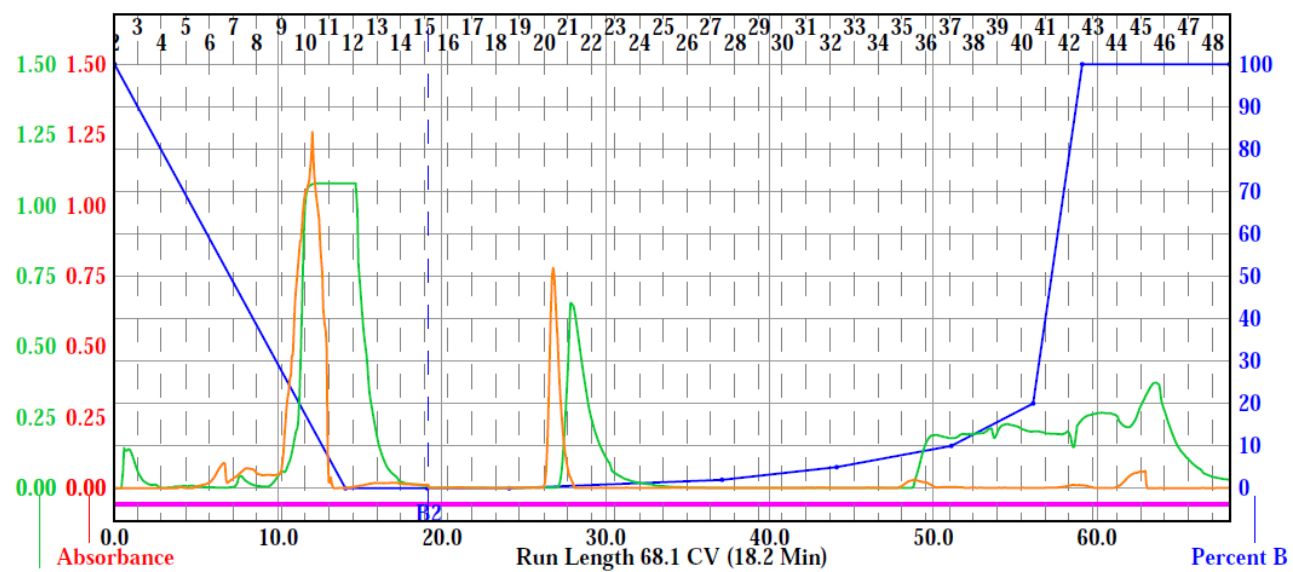


Table 2: Sample ID, bioassay data, and weight obtained for flash chromatography from MSX 68425. All data is percent survival of cell line. (sm = starting material prior to fractionation)

Sample ID	Conc.	MCF-7wtk	H460	SF268	Amount (mg)
01007-33-sm	20 µg/mL	31.7	13.7	45.5	
	2 µg/mL	98.9	91.6	97.5	
01007-33-1	20 µg/mL	105.3	101.0	108.3	2.1
	2 µg/mL	102.4	106.1	105.1	
01007-33-2	20 µg/mL	30.4	11.5	44.3	167.4
	2 µg/mL	100.2	93.7	94.8	
01007-33-3	20 µg/mL	49.2	42.6	63.1	26.6
	2 µg/mL	100.5	99.9	108.6	
01007-33-4	20 µg/mL	69.2	84.9	94.4	30.1
	2 µg/mL	102.0	109.3	113.7	
01007-33-5	20 µg/mL	90.4	82.0	73.6	22.9
	2 µg/mL	100.1	105.5	108.7	

D. Purification and Analysis

Active fractions were analyzed via RP-HPLC (figure 9) for establishment of a gradient for use with preparative HPLC. The fractions are then purified (>95%) by preparative-HPLC (figure 10) and pooled based on the UV chromatogram and PDA profiles to isolate the compounds. Purified fractions are submitted for further bioassay testing to verify activity in the fraction (table 3) and then analyzed by Nuclear Magnetic Resonance Spectroscopy (NMR) and High Resolution Mass Spectrometry (HRMS) for chemical structure elucidation.

Figure 9: Analytical HPLC chromatogram of 01007-33-2 @230 nm.

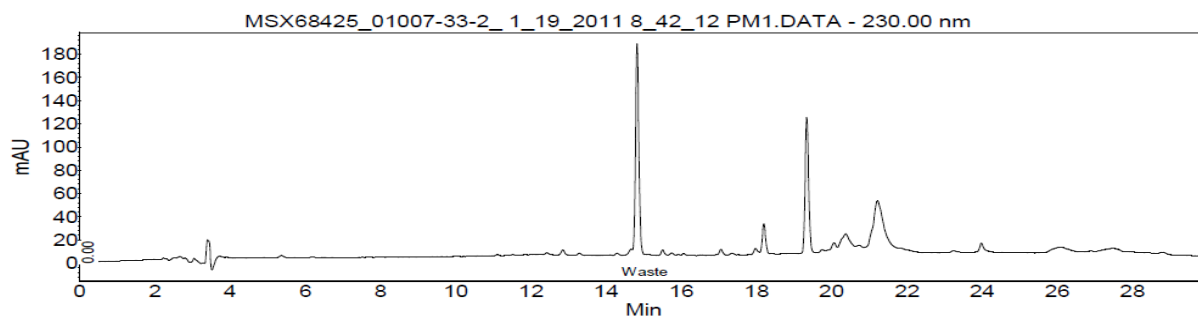
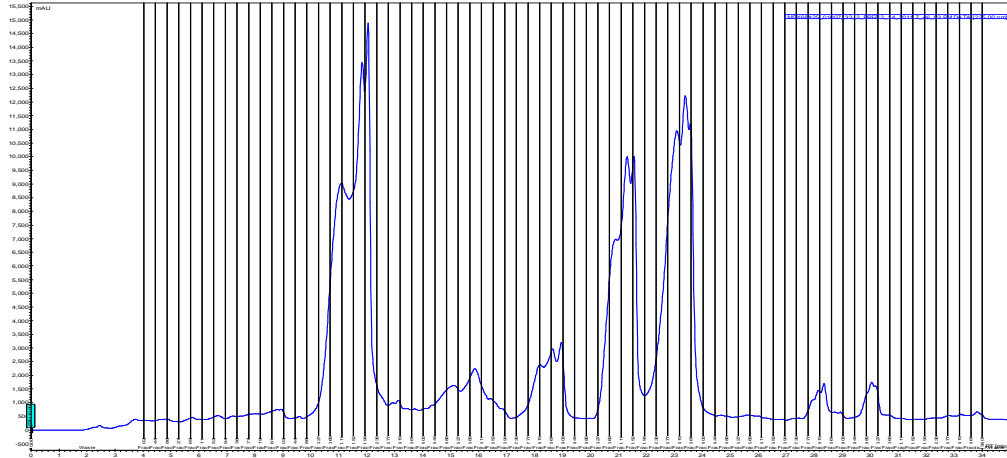


Figure 10: a) Preparative HPLC of 01007-33-2 (vertical black bars represent fractions) and b) pooling based on chromatogram

a)



b)

Sample ID	Pooled Fractions	Wt. (mg)
01007-150-1	14-24	10.2
01007-150-2	27-31	5.0
01007-150-3	32-37	5.8
01007-150-4	39-43	7.0
01007-150-5	44-49	11.0

Table 3: Bioassay data for fractions of 01007-33-2 (renamed 01007-150). Numbers are % survival. A survival rate of <20% for the 20 µg/mL concentration is considered active.

Sample ID	Conc.	MCF-7	H460	SF268
01007-150-sm	20 µg/mL	41.9	30.6	31.8
	2 µg/mL	84.6	115.3	95.1
01007-150-1	20 µg/mL	48.7	80.9	89.6
	2 µg/mL	93.3	103.6	91.6
01007-150-2	20 µg/mL	39.6	14.1	37.6
	2 µg/mL	102.8	108.2	97.8
01007-150-3	20 µg/mL	30.3	7.1	23.0
	2 µg/mL	117.3	98.7	92.6
01007-150-4	20 µg/mL	10.8	0.7	10.2
	2 µg/mL	26.6	8.5	33.1
01007-150-5	20 µg/mL	19.7	8.1	24.8
	2 µg/mL	71.0	69.2	71.8

E. Human Cancer Cell Panel

The human cancer cell panel growth and testing were conducted at the department of pharmaceutical sciences at North Carolina Central University in Durham, NC in the laboratory of Dr. David J. Kroll. Initial crude extract, fractionations, and prep-HPLC bioassays were at concentrations of 20 µg/mL and 2 µg/mL. EC₅₀ values were obtained by serially diluting the concentration (µM) in half log steps. All samples were dissolved in DMSO and the final concentration was ≤ 0.5%.

The human cancer cell panel consisted of MCF-7 human breast carcinoma (Barbara A. Karmanos Cancer Center, Detroit, MI), NCI-H460 human non-small cell lung carcinoma (American Type Culture Collection, Manassas, VA), and SF-268 human astrocytoma (NCI Developmental Therapeutics Program, Frederick, MD). All cell lines were adapted and maintained RPMI-1640 medium supplemented with fetal bovine serum at 10% (v/v), 100 U/mL penicillin G, and 100 µg/mL streptomycin sulfate. The atmosphere was maintained at 5% CO₂ and 37 C. Cells were used in the logarithmic growth phase. Cell suspensions were prepared at densities of 3,000 (MCF-7), 1,500 (H460), and 10,000 (SF-268) cells/50 µL of medium.³² The assay was monitored at the UV maximum of 562 nm.¹²

CHAPTER VII

RESULTS

The crude extract of the small scale fermentation of MSX 68425 showed moderate activity in the human cancer cell panel as evidenced by ~10% cell survival of H460 cells when tested at 20 $\mu\text{g/mL}$. The crude extract was fractionated via normal phase flash chromatography, and the resultant pools were tested in the human cancer cell line panel. The second pool showed activity that was slightly more potent than the crude extract and was then subjected to preparatory scale HPLC for purification of the compounds. The numbering of the isolated compounds (**1 – 3**) relates to their order of elution in RP-HPLC purification of fraction 01007-33-2.

A. 01007-150-1 (Compound 1)

01007-150-1 (figure 11) was isolated after one round of prep-HPLC with a purity >95%, verified via UPLC (Figure 12). A comparison of the UV data (λ_{max} 233, 259, 293, and 374 nm) showed that the three isolated compounds were closely related, and this was confirmed by ^1H NMR data, as the chemical shifts and splitting in the aromatic region (δ_{H} 6.7-7.6) were highly similar (see table 4). Dereplication of the compounds was attempted by inputting the HRMS and UV data ($\pm 10\text{nm}$) into the Dictionary of Natural Products database (DNP ver. 20.1); no matches were found.

Compound **1** was a yellow crystalline solid, which is characteristic of xanthenes. The HRMS data was $m/z = 287.09070$ $[\text{M} + \text{H}]^+$ with a second mass peak at $m/z = 269.08011$ $[(\text{M} - \text{H}_2\text{O}) + \text{H}]^+$, denoting a loss of H_2O ($m/z = 18$). Using the HRMS data,

a chemical formula of $C_{16}H_{14}O_5$ was calculated, corresponding to an Index of Hydrogen Deficiency (IHD) of 10. The ^{13}C NMR (figure 14) data showed twelve peaks in the aromatic region, with eight of those being quaternary carbons, and a peak at δ_C 184 denoting a ketone. These results were combined with 1H NMR data (figure 13), which showed four aromatic protons H-2 (δ_H 6.8), H-3 (δ_H 7.6), H-4 (δ_H 6.9), and H-8 (δ_H 7.3), helping to confirm that the backbone of **1** was a tetra substituted xanthone. The substituents were determined from the 1H NMR data as phenol (δ_H 12.6), hydroxymethyl [δ_H 5.0 (CH_2) and δ_H 4.5 (-OH)], methoxy (δ_H 3.8), and methyl (δ_H 2.5) groups.

The positions of the substituents and aromatic protons were determined by 2D-NMR. The three 2D-NMR experiments utilized here were: COSY (Correlation spectroscopy, 1H - 1H correlations of adjacent protons), HSQC-edited (Heteronuclear single quantum coherence, direct 1H - ^{13}C connectivity phase edited giving results similar to DEPT-135 ^{13}C NMR), and HMBC (Heteronuclear multiple bond correlation, long range (2-4 bonds, 3 typically) 1H - ^{13}C correlations). Only one spin system was observed in the COSY spectrum (figure 15) for the correlations between H-2 (δ_H 6.8), H-3 (δ_H 7.6), and H-4 (δ_H 6.9). In the HSQC-edited NMR experiment (figure 16), the aromatic protons at δ_H 7.6 (H-3), δ_H 6.9 (H-2), and δ_H 6.8 (H-4) correlated to the carbon signals at δ_C 137.0 (C-3), δ_C 110.6 (C-2), and δ_C 106.7 (C-4), respectively. In the HMBC experiment (figure 17), the proton at δ_H 7.3 (H-8) correlated to the methyl group at δ_C 17.5 (C-12), the carbon at δ_C 153.8 (C-6), and the carbonyl at δ_C 184.5 (C-9). The methoxy proton at δ_H 3.8 (H-11) showed a correlation in the HMBC spectrum to the quaternary carbon at C-6. The hydroxymethyl $-CH_2-$ proton at δ_H 5.0 (H-10) correlated to the quaternary carbon at C-6 as well, denoting its position on C-5. The phenolic proton signal at δ_H 12.6 was determined to be on C-1 by the HMBC correlations to the carbon at δ_C 110.6 (C-2) and

δ_c 109.2 (C-9a). Compound **1** was determined to be a new xanthone, and was assigned the systematic name 1-hydroxy-5-(hydroxymethyl)-6-methoxy-7-methyl-xanthone.

Figure 11: Proposed structure of compound **1** (01007-150-1)

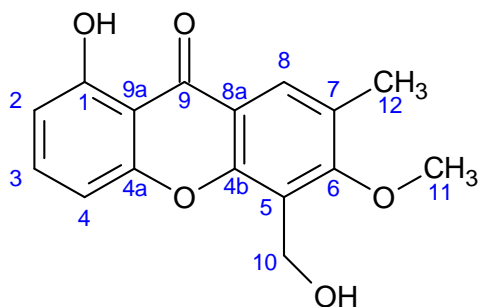


Figure 12: UPLC @ 235 nm of compound **1** (01007-150-1) showing >95% purity

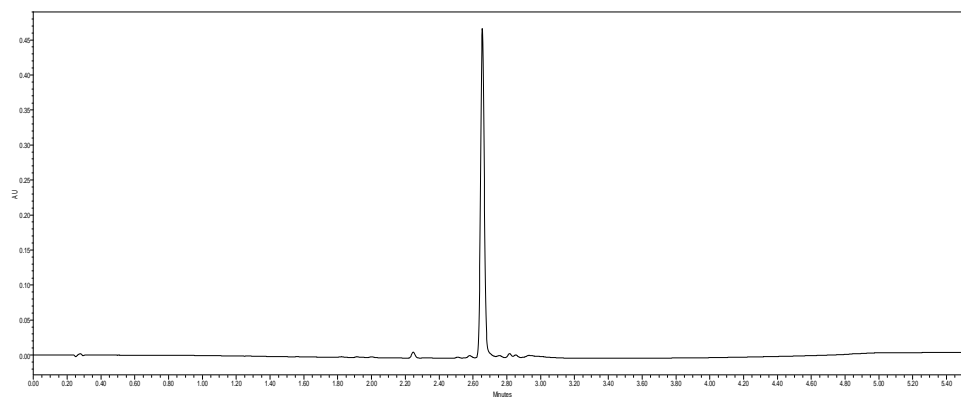


Figure 13: ^1H NMR of Compound 1 (CDCl_3) and expansion of aromatic region (δ_{H} 6.5-7.0) (inset)

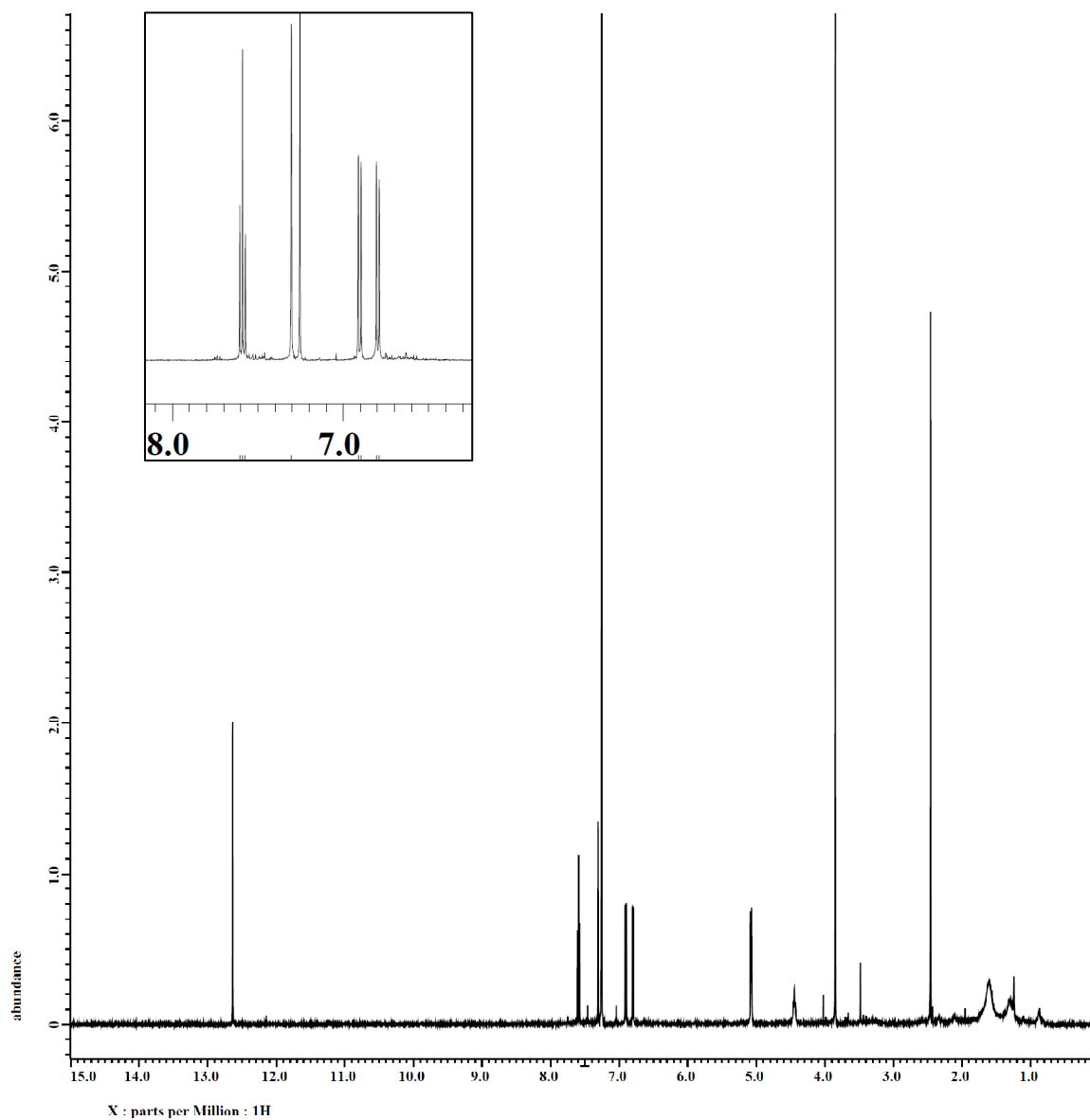


Figure 14: ^{13}C NMR data of compound 1

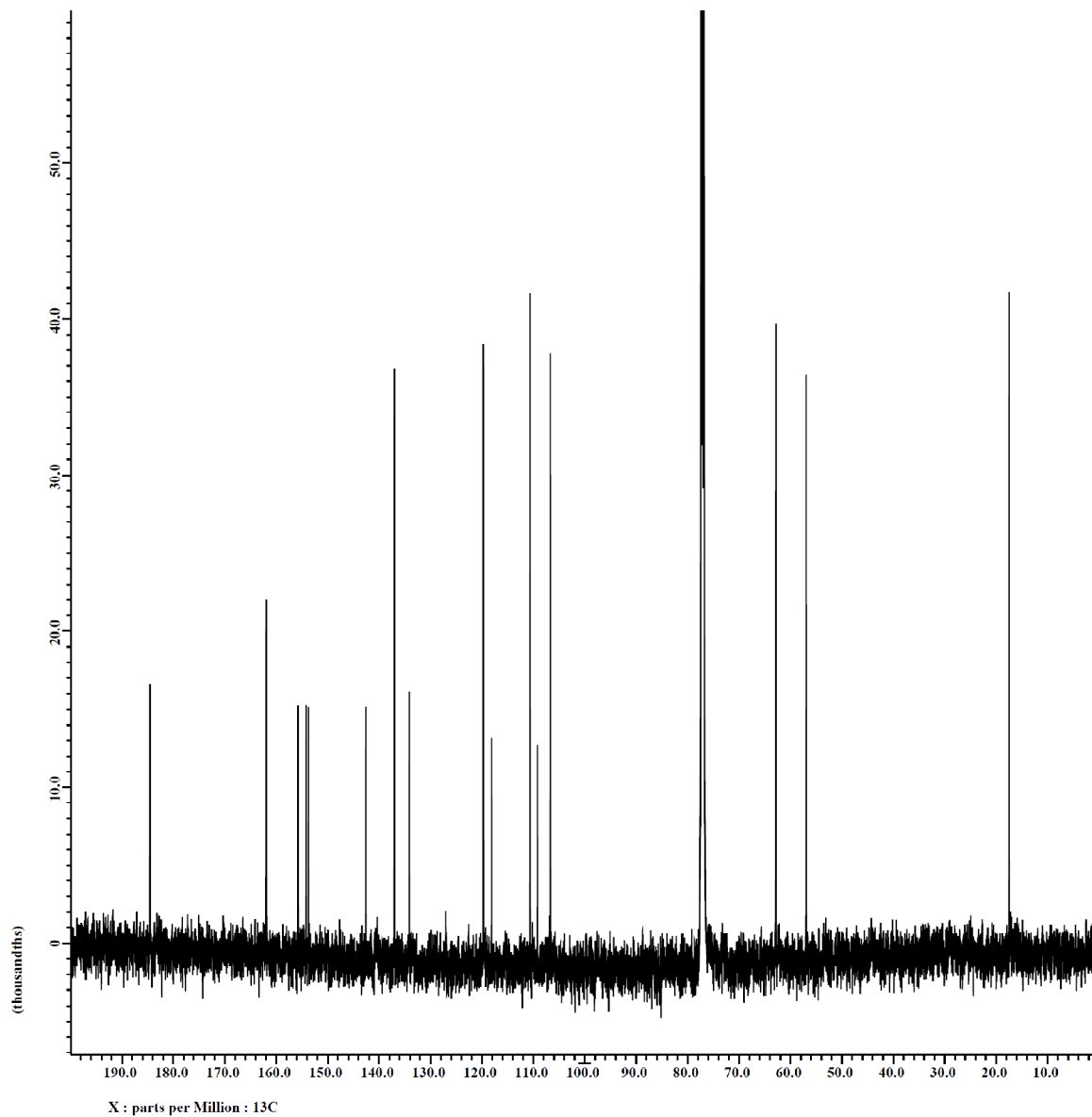


Figure 15: COSY NMR data of Compound 1

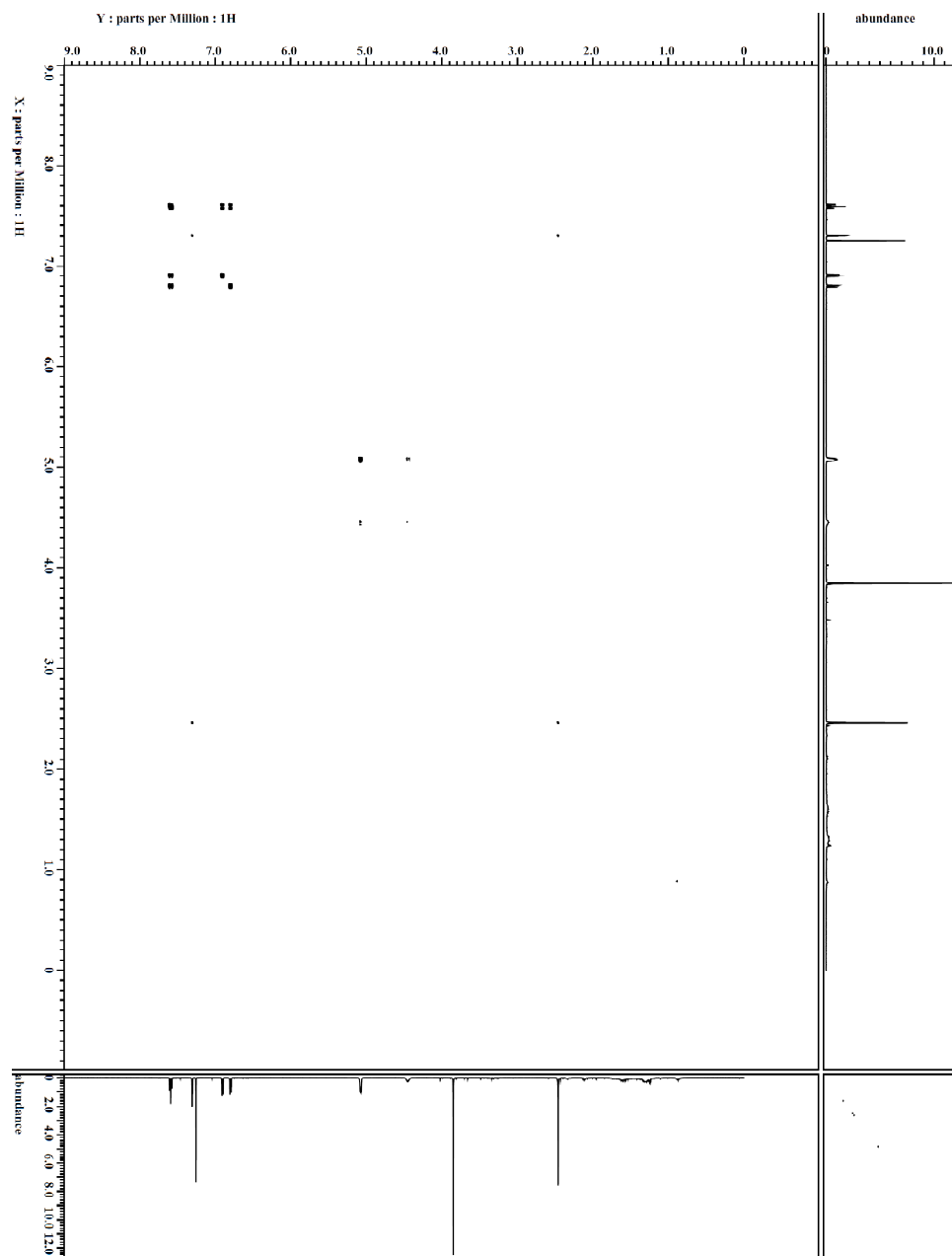


Figure 16: HSQC-edited NMR data of Compound 1

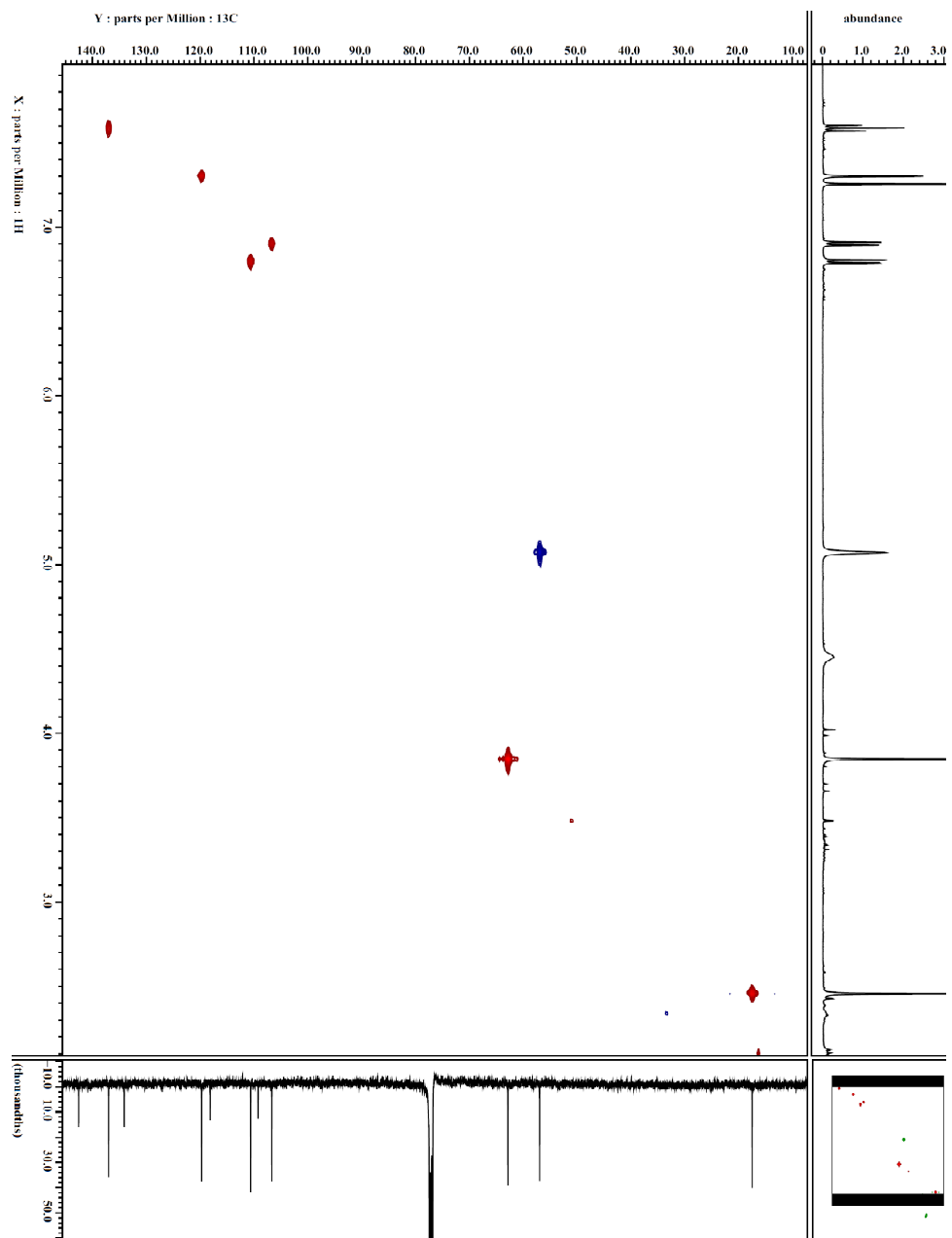


Figure 17: HMBC NMR data of Compound 1

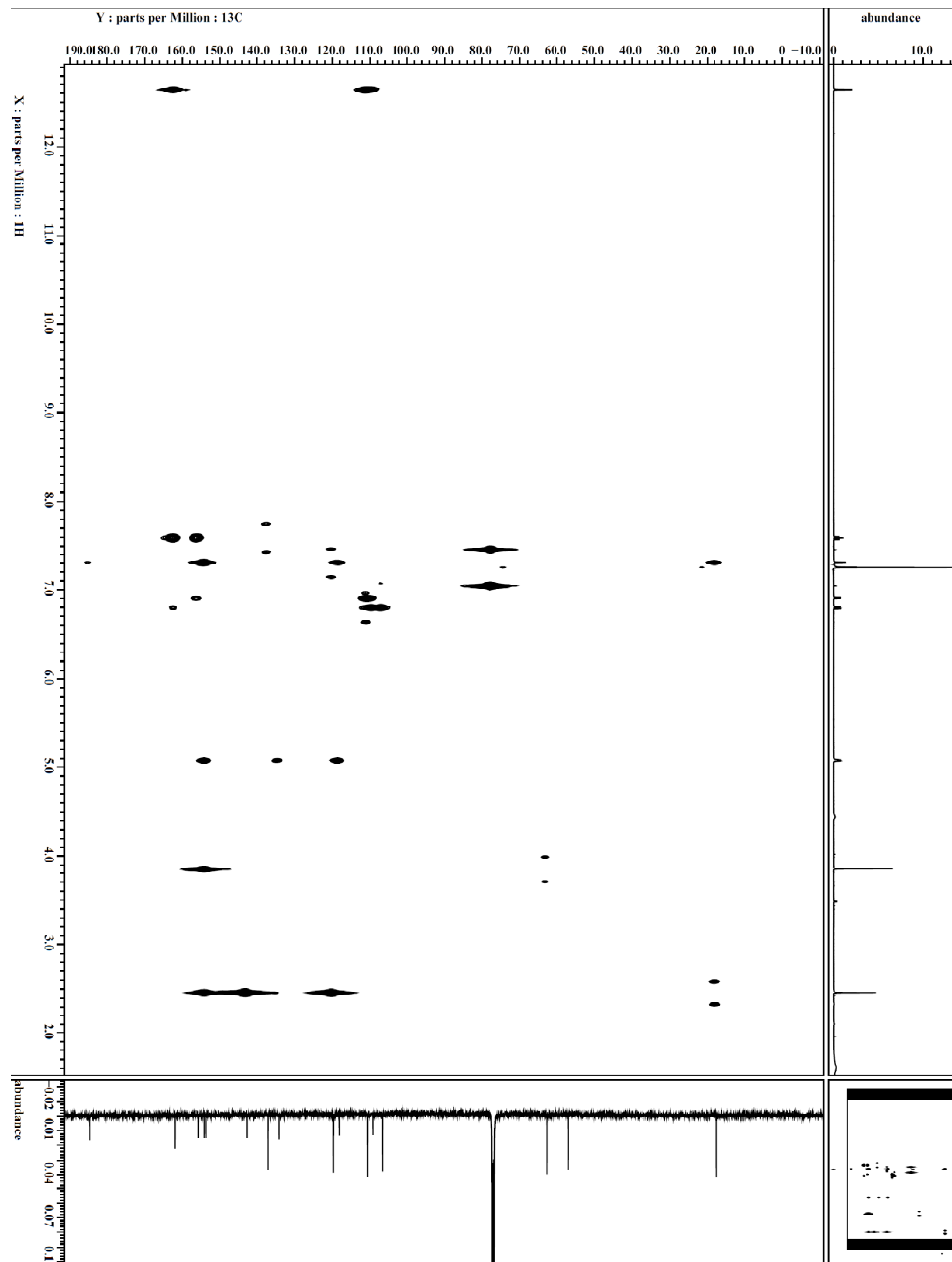


Table 4: NMR data table for compounds (**1** – **3**). ¹³C data for **2** is inferred from HSQC and HMBC spectra.

Position	Compound 1		Compound 2		Compound 3	
	δ_{H} Mult (J in Hz)	δ_{C}	δ_{H} Mult (J in Hz)	δ_{C}	δ_{H} Mult (J in Hz)	δ_{C}
1		161.9		162.2		162.2
2	6.9 d 8	106.7	6.8 d 8	108.0	6.8 d 8	106.3
3	7.6 t 8	137.0	7.6 t 8	136.4	7.5 t 8	136.1
4	6.8 d 8	110.6	6.9 d 8	110.4	6.7 d 8	110.1
4a		155.7		156.7		155.7
4b		154.1		151.5		153.4
5		134.1	7.5 s	103.0		133.1
6		153.8		155.4		153.9
7		142.6		138.7		140.8
8	7.3 s	119.7	7.3 s	120.0	7.1 s	117.2
8a		118.1		119.5		118.0
9a		109.2		109.0		109.4
9		184.5		182.6		184.6
10	5.0 s	56.9			2.8 s	14.7
11	3.8 s	62.8	3.9 s	56.0	3.7 s	60.4
12	2.5 s	17.5	2.4 s	17.8	2.4 s	17.3
1-OH	12.6 s		12.8 s		13.0 s	
10-OH	4.5 bs					

B. 01007-150-3 (Compound 2)

Compound 2 (figure 18) was purified to >95% purity by several rounds of prep-HPLC. The UV (λ_{max} 235, 269, 290, and 380 nm) and mass spectrometry data of **2** were found to be similar to **1**. The key difference from the latter was a molecular ion ($m/z = 257.08026$ [M + H]⁺), corresponding to a molecular formula of C₁₅H₁₃O₄ and an IHD of 10, that was 30 mass units different than **1**, suggesting the absence of a –CH₂-O- moiety.

Due to a paucity of sample this compound was analyzed utilizing a capNMR probe, and the ¹³C assignments were extrapolated from the HSQC and HMBC experiments. The alteration of the substituents was verified by the ¹H capNMR data (figure 19), showing the absence of the hydroxymethyl group and the presence of an additional proton in the aromatic region (H-5 δ_{H} 7.5). The signals for the phenol at C-1 (H-1 δ_{H} 12.7), methoxy at C-6 (H-11 δ_{H} 3.9), and methyl at C-7 (H-12 δ_{H} 2.4) were present in the ¹H NMR spectra, helping to confirm the similarity of compounds **1** and **2**. The HSQC NMR data (figure 21) showed the additional ¹H-¹³C correlation of the proton at position 5. HMBC correlations (figure 22) were also present from the proton at H-5 (δ_{H} 7.5) to the carbons at C-6 (δ_{C} 155.4), C-7 (δ_{C} 138.7), and C-4b (δ_{C} 151.4). Compound **2** was determined to be a new xanthone, and was assigned the systematic name 1-hydroxy-6-methoxy-7-methyl-xanthone.

Figure 18: Proposed structure of 01007-150-3 Compound **2**

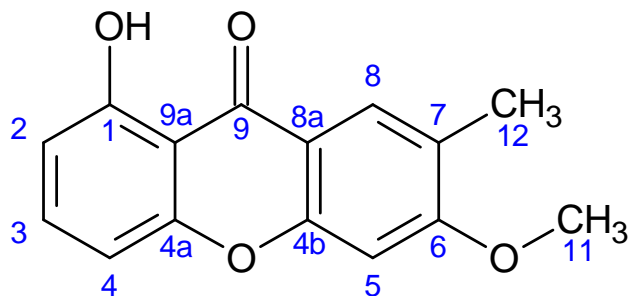


Figure 19: UPLC of Compound **2** @235 nm showing >95% purity.

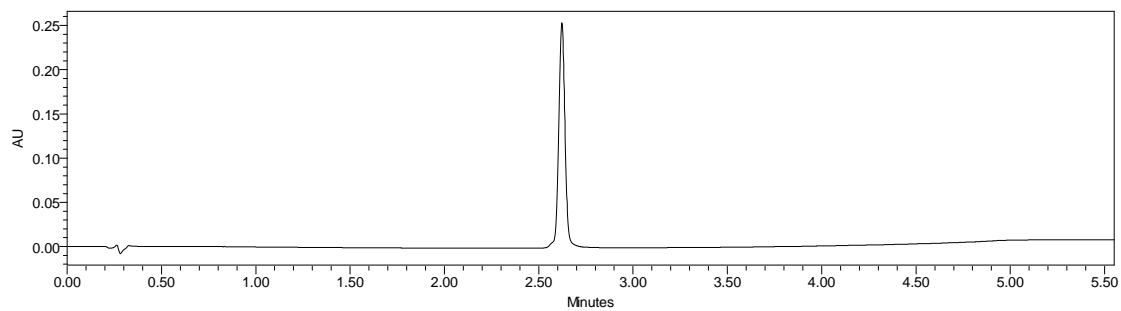


Figure 20: ^1H capNMR spectrum for Compound **2** (CDCl_3) and expansion of aromatic region (δ_{H} 6.5-8.0) (inset)

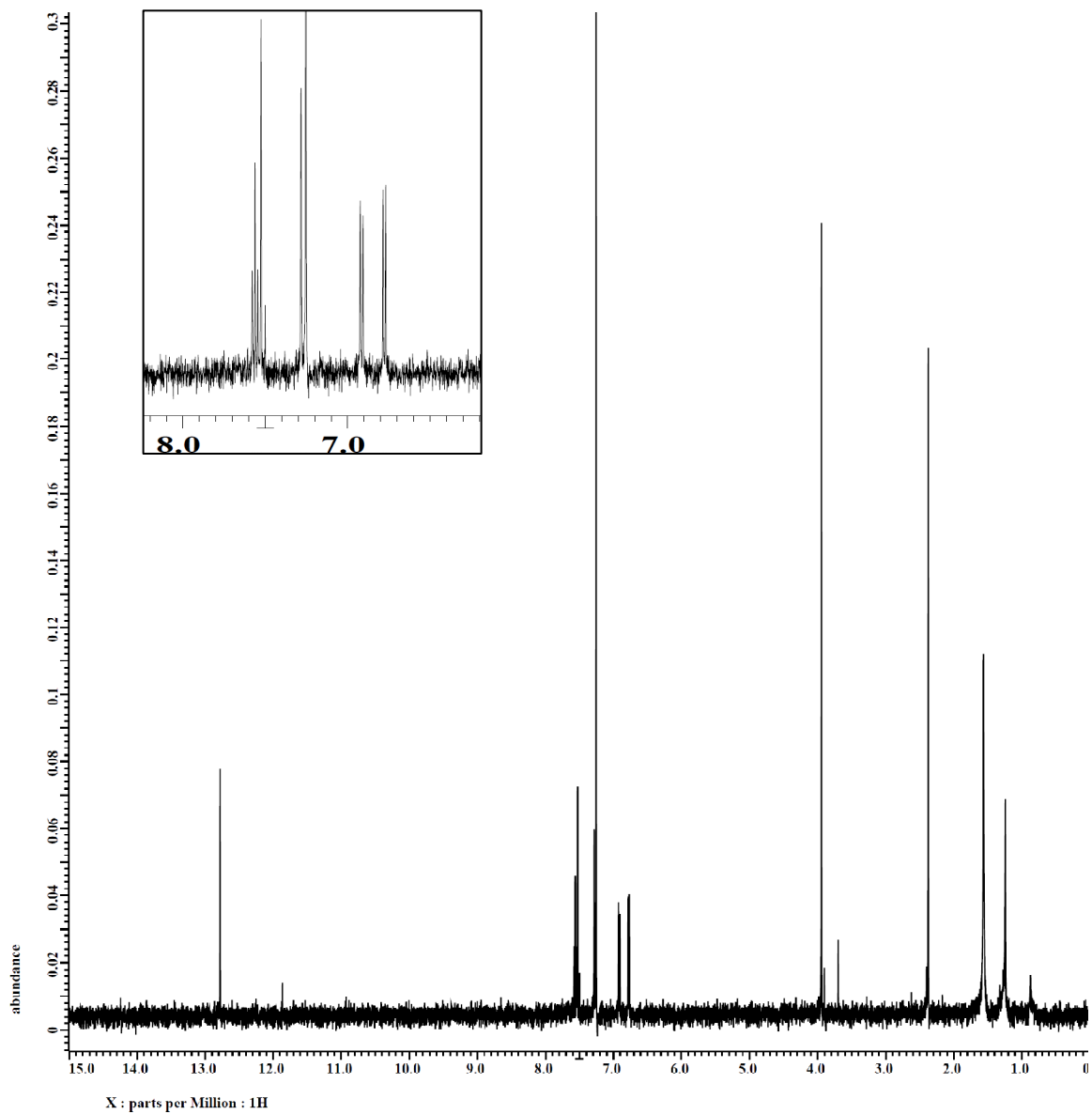


Figure 21: HSQC-edited spectrum of compound **2** (CDCl₃, CapNMR)

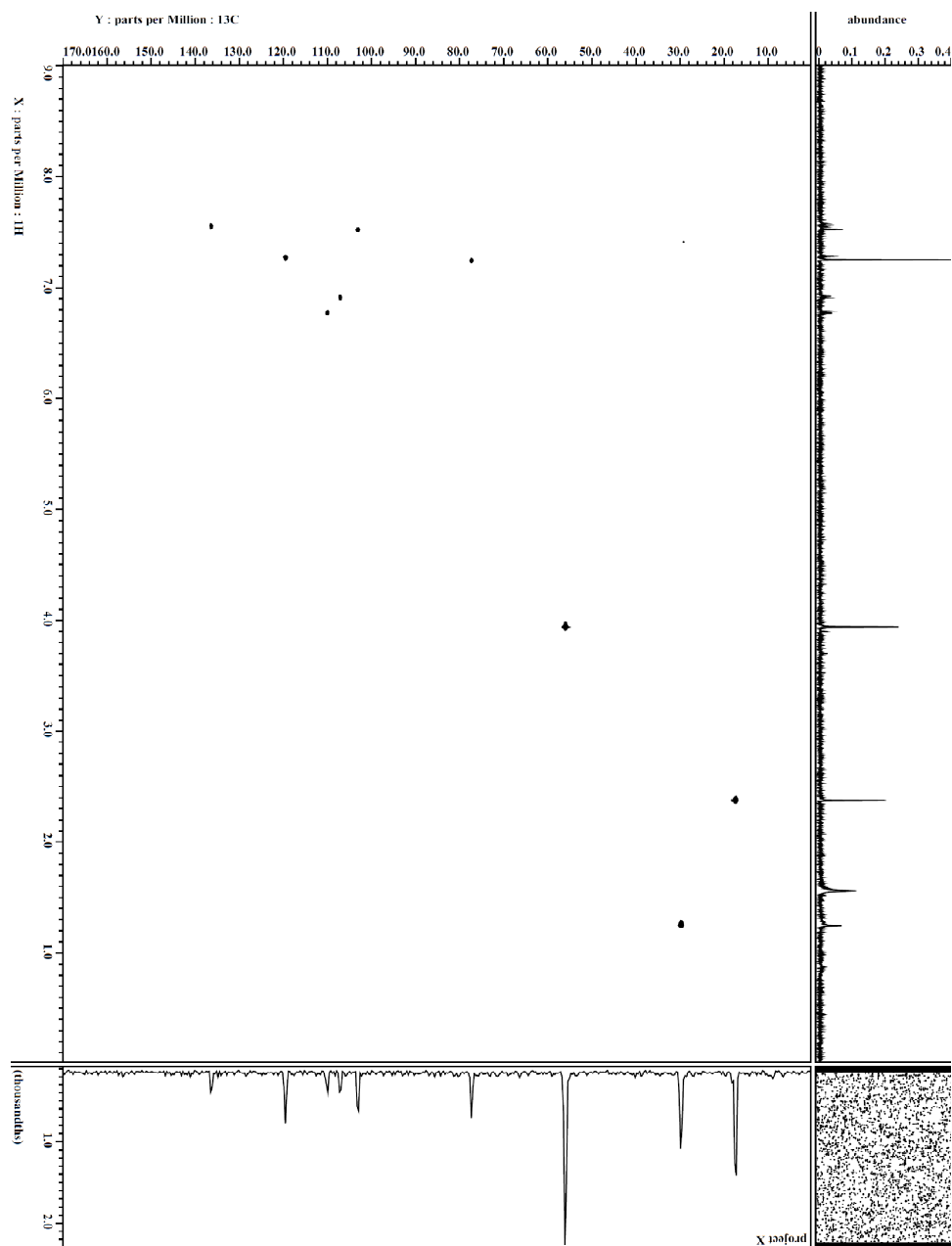
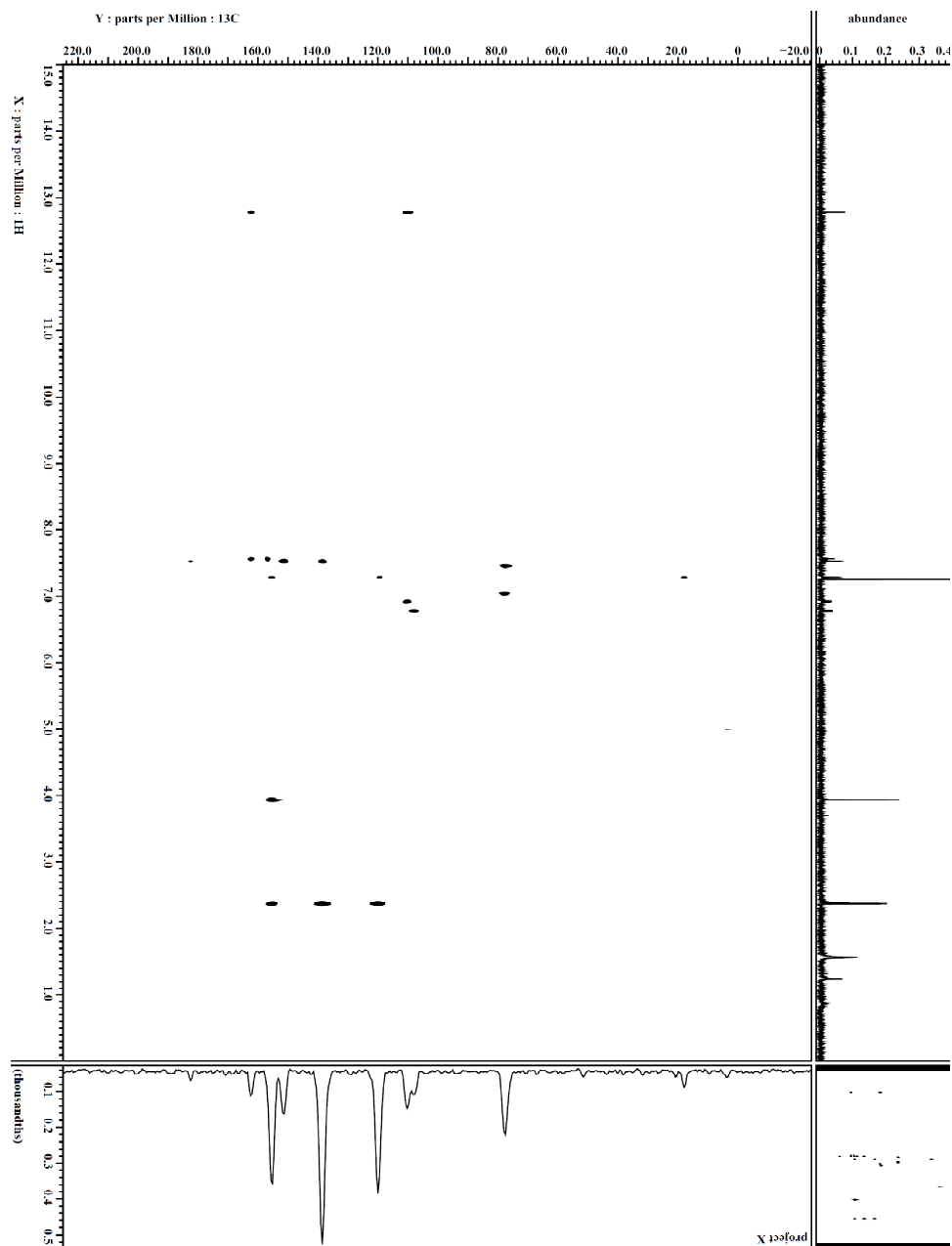


Figure 22: HMBC spectrum of compound **2** (CDCl₃, CapNMR)



C. 01007-150-4 (Compound 3)

Compound **3** (figure 23) was purified to >95% (figure 24) by a single round of prep-HPLC. The UV (λ_{max} 234, 256, 287, and 369 nm) and mass spec data showed that **3** was similar to **1**. The mass spec data ($m/z = 271.09586$ [M + H]⁺) corresponded to a chemical formula of C₁₆H₁₄O₄ and an IHD of 10. Comparison of the HRMS data between **1** and **3** showed the difference of mass to equal that of an oxygen atom. This was confirmed through the ¹H NMR data (figure 25) that showed the absence of the -CH₂-O- moiety, and the presence of an additional singlet in the upfield region δ_{H} 2.8 (H-10) of the spectrum. The ¹³C data (figure 26) confirmed the presence of an additional methyl group at δ_{C} 14.6 (C-10). The proton signals for the phenol at C-1 (H-1 δ_{H} 13.0), methoxy group at C-6 (H-11 δ_{H} 3.7), and methyl group at C-7 (H-12 δ_{H} 2.4) were present in the ¹H NMR spectrum. The additional upfield proton signal was determined to be a methyl group at the C-5 position. 2D NMR was utilized to confirm the positions of the methyl groups and assignment of the ¹³C and ¹H NMR signals. The HSQC-edited experiment (figure 27) showed the correlation of the methyl group attached to position C-5 of the xanthone ($\delta_{\text{H-10}}/\delta_{\text{C-10}} = 2.8/14.7$) and the C-7 methyl group ($\delta_{\text{H-12}}/\delta_{\text{C-12}} = 2.4/17.3$). In the HMBC experiment (figure 28), the methyl proton at H-10 (δ_{H} 2.8) correlated to C-6 (δ_{C} 153.9) and C-4b (δ_{C} 153.4) confirming its position at C-5. Compound **3** was determined to be a new xanthone and was assigned the systematic name 1-hydroxy-5,7-dimethyl-6-methoxy-xanthone.

Figure 23: Proposed structure of 01007-150-4 Compound **3**

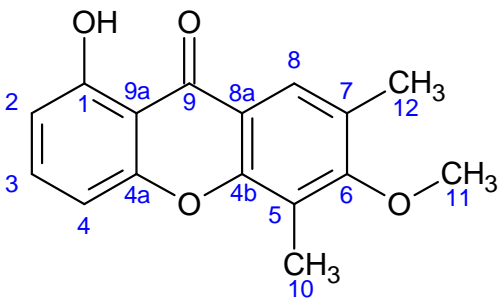


Figure 24: UPLC of Compound **3** (01007-150-4) showing >95% purity.

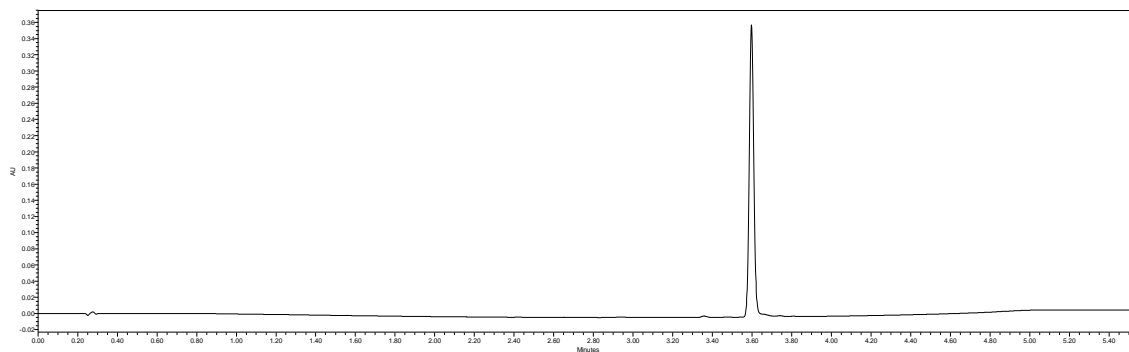


Figure 25: ^1H NMR data for Compound **3** (CDCl_3) and expansion of aromatic region (δ_{H} 6.5-8.0) (inset)

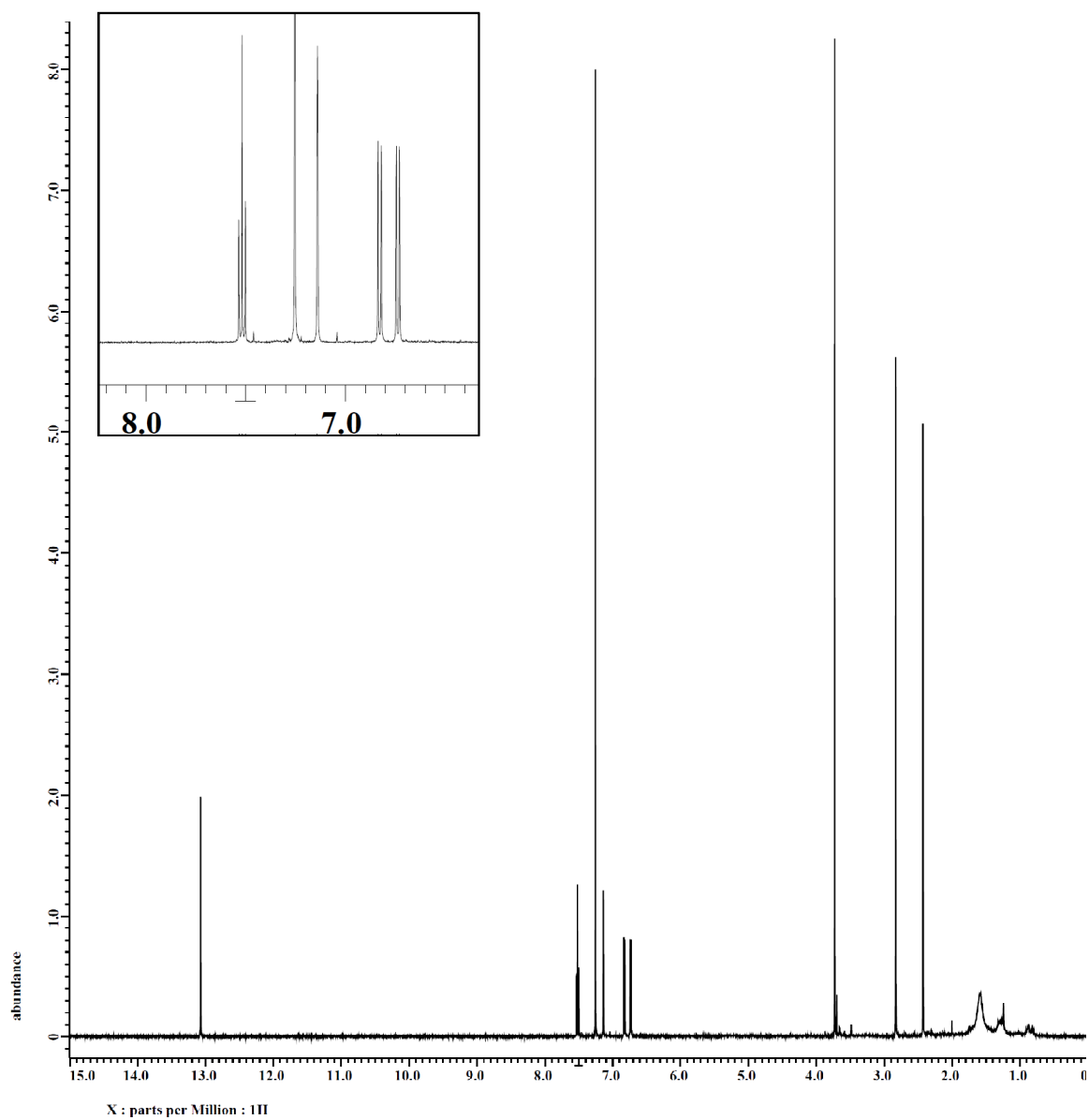


Figure 26: ^{13}C NMR of Compound **3** in CDCl_3 (01007-150-4)

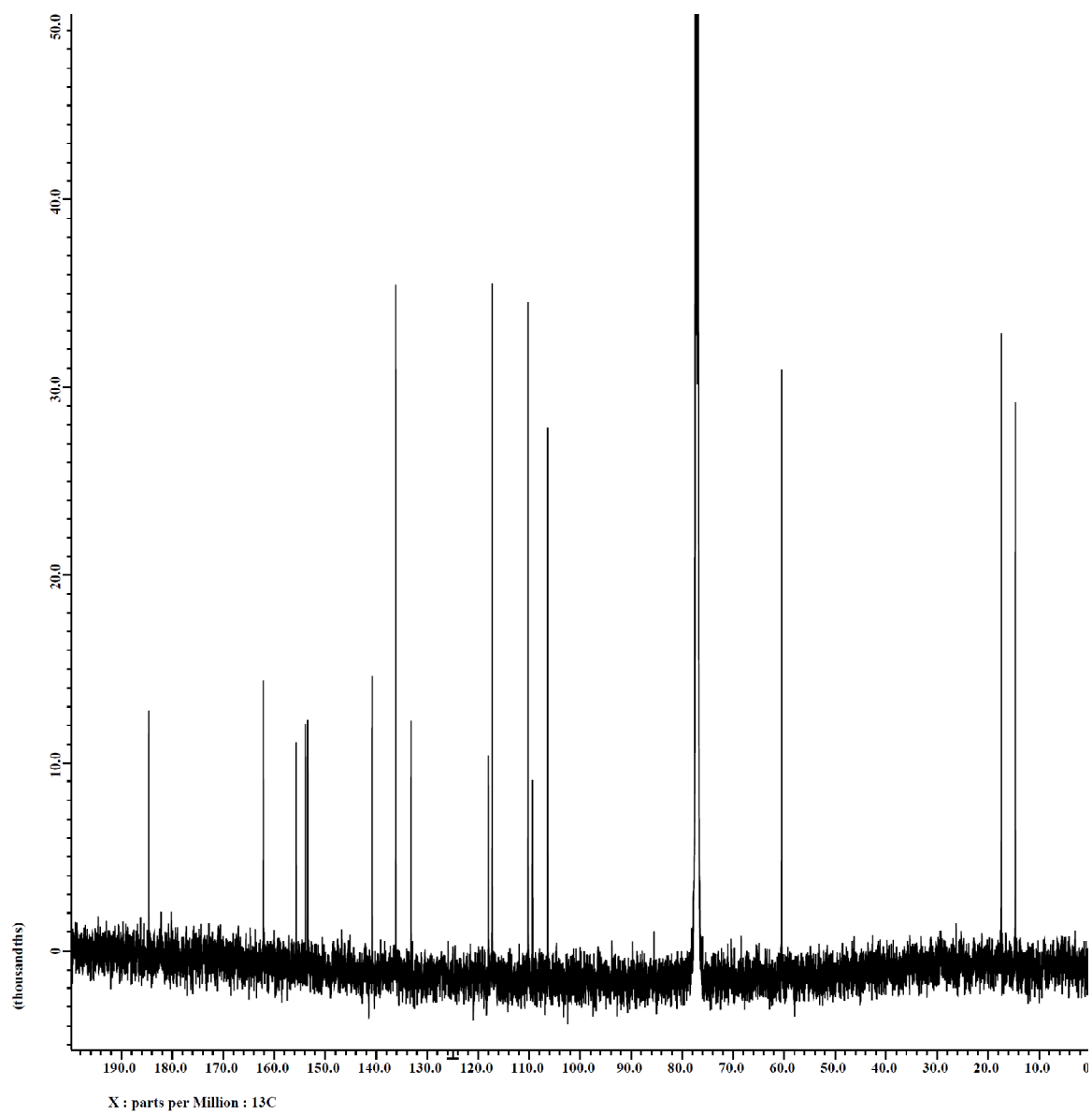


Figure 27: HSQC-edited spectrum of Compound 3 (01007-150-4)

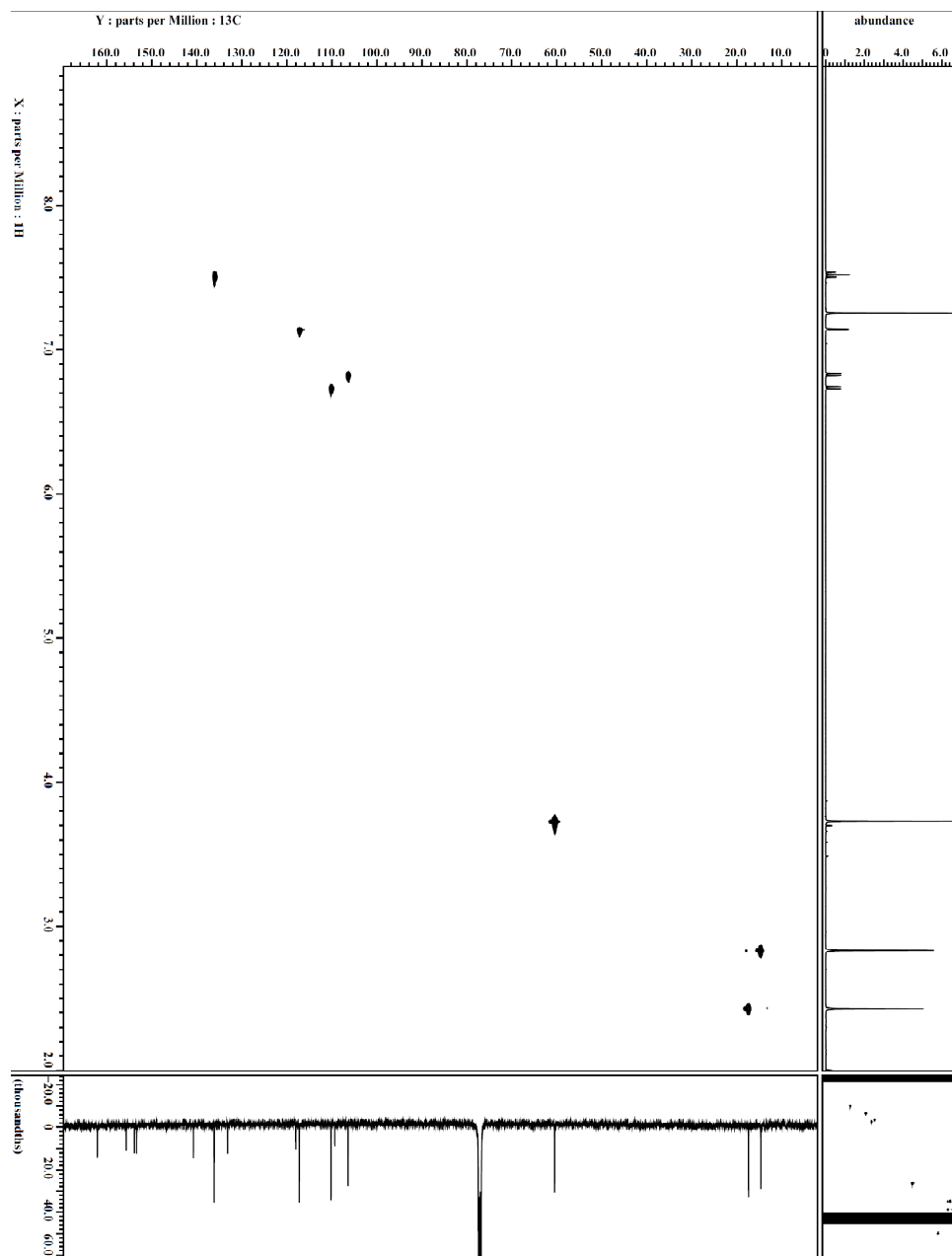
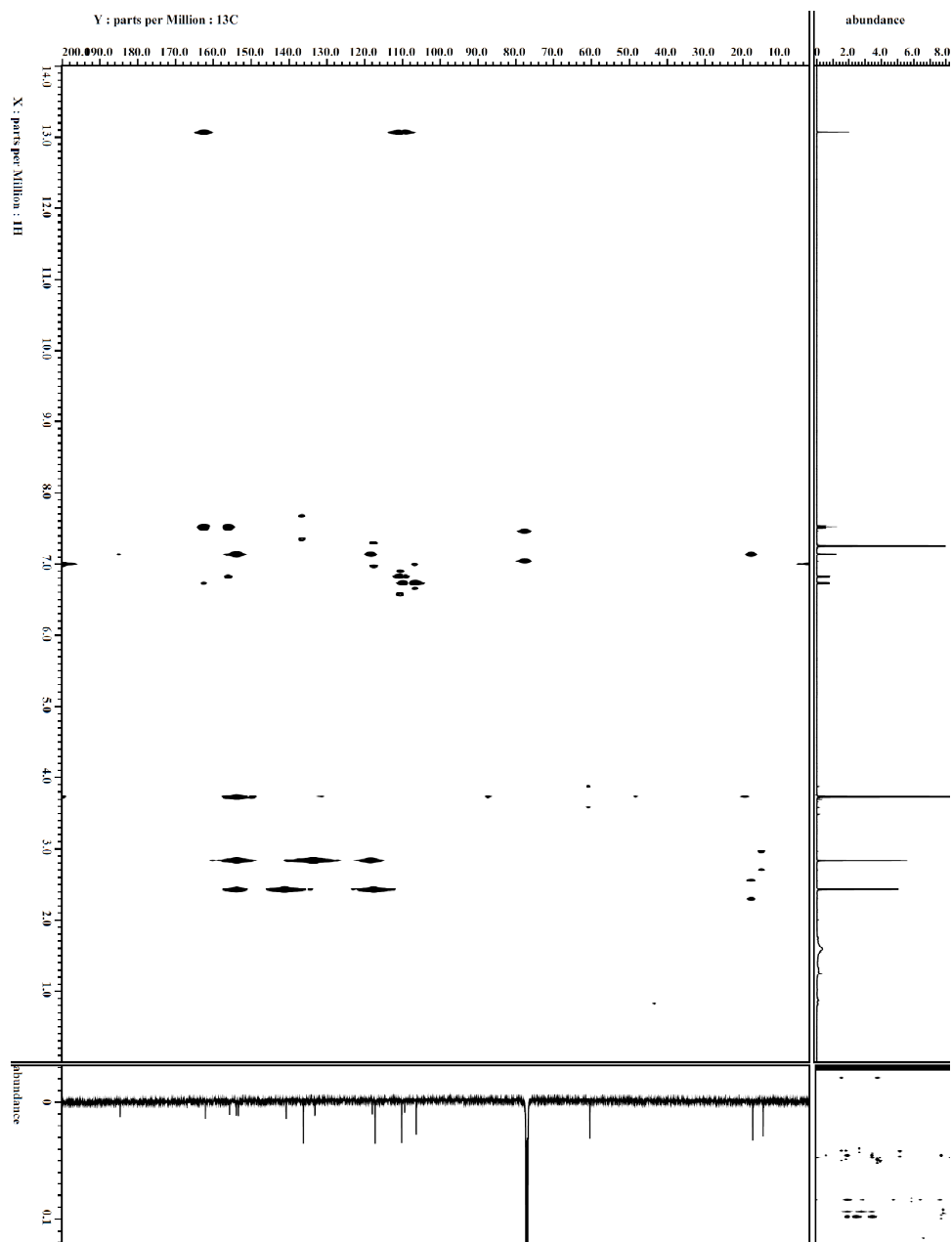


Figure 28: HMBC spectrum of Compound 3 (01007-150-4)



D. EC₅₀

The EC₅₀ of all three compounds was evaluated. The assay was performed at North Carolina Central University. The assay was performed as a serial dilution to obtain 50% growth inhibition of the cancer cell line. This assay was performed with a positive control of camptothecin, a known and commercially used chemotherapeutic agent. The results are reported in μM .

Table 5: EC₅₀ bioassay data. All results in μM .

	EC ₅₀ (μM)		
	MCF-7	H460	SF268
Camptothecin	0.15	0.01	0.07
Compound 1	100	58.3	100
Compound 2	100	100	100
Compound 3	100	59.6	100

CHAPTER VIII

CONCLUSION

Using the method of bioactivity-directed fractionation, three new xanthenes were isolated and their structures elucidated via a suite of spectroscopic and spectrometric techniques. The xanthone backbone has been well described in the literature due to its prevalence in nature, but the continuing discovery of new xanthenes points to the diversity of the substituents found on the xanthone backbone. The fungus (MSX 68425) biosynthesized xanthenes (**1** - **3**) that were altered only at the C-5 position, which had an effect on the cytotoxicity of the compounds with the methyl group or hydroxymethyl at C-5 (compounds **1** and **3**) being more potent than the non-substituted compound at the same position (compound **2**).

REFERENCES

- 1) Bush, K. *ASM News* **2004**. 70. 282–287.
- 2) Hawkey, P.M. *J. Antimicrob. Chemother.* **2008**. 62, i1–i9
- 3) Falkinham, JO, Wall, TE, Tanner, JR, Tawaha, K, Alali, FQ, Li, C, Oberlies, NH. *Appl. Environ. Microbiol.* **2009**, 75: 2735-2741
- 4) Hageman, J. C.; T. M. Uyeki; J. S. Francis; D. B. Jernigan; J. G. Wheeler; C. B. Bridges; S. J. Barenkamp; D. M. Sievert; A. Srinivasan; M. C. Doherty; L. K. McDougal; G. E. Killgore; U. A. Lopatin; R. Coffman; J. K. Mac-Donald; S. K. McAllister; G. E. Fosheim; J. B. Patel; L. C. McDonald. *Emerg. Infect. Dis.* **2006**. 12, 894–899.
- 5) Spizek, J.; Nvotna, J.; Rezanka, T.; Demain, A. *J. Ind. Microbiol. Biotechnol.* **2010**. 37, 1241-1248
- 6) Thomas, C.M.; Nielsen, K.M. *Nat. Rev. Microbiol.* **2005**. 3, 711–721
- 7) Lee, J. C.; Park, H. R.; Park, D. J.; Lee, H. B.; Kim, Y. B.; and Kim, C. J. *Let. App. Micro.* **2003**, 37, 196-200.
- 8) Jin, Z.H.; Wang, M.R.; Cen, P.L. *Appl. Microbio. Biot.* **2002**. 58, 63–66.
- 9) Gastaldo, L.; Marinelli, C.; Restelli, E.; Quarta, C. *J. Indust. Microbiol.* **1996**. 16, 305-308
- 10) Marshall, VP; S. J. McWethy, J. Visser, J. L. Cialdella, A. L. Laborde. *Dev. Ind. Microbiol.* **1987**. 28, 105-114.
- 11) Hackmann, C. *Zeitschr. f. Krebsforsch.* **1954**. 60, 250-255.
- 12) Li, C.; Lee, D.; Graf, T. N.; Phifer, S. S.; Nakanishi, Y.; Riswan, S.; Setyowati, F. M.; Saribi, A. M.; Soejarto, D. D.; Farnsworth, N. R.; Falkinham, J. O., III; Kroll, D. J.; Kinghorn, A. D.; Wani, M. C.; Oberlies, N. H. *J. Nat. Prod.* **2009**, 72, 1949–1953.
- 13) Cain, C. C., A. T. Henry, R. H. Waldo III, L. J. Casida, Jr., and J. O. Falkinham III. *Appl. Environ. Microbiol.* **2000**. 66:4139–4141.
- 14) American Cancer Society. 2010. Cancer Facts and Figures 2010.
- 15) Jemal, A.; Bray, F.; Center, M.M.; Ferlay, J.; Ward, E.; Forman, D. *Cancer J Clin.* **2011**. 61, 69-90.
- 16) Johnson IS, Armstrong JG, Gorman M, Burnett JP. *Cancer Res* **1963**. 23 (8 Part 1): 1390–1427.
- 17) Wall, M. E., Wani, M. C., Cook, C. E., Palmer, K. H., McPhall, A. T., Sim, G. A. *J. Amer. Chem. Soc.* **1966**. 88, 3888-3890.

- 18) Wani, M. C., Taylor, H. L., Wall, M. E., Coggan, P., McPhall, A. T. *J. Amer. Chem. Soc.* **1971**, 93, 2325-2327.
- 19) Newman, D. J. and Cragg, G.M. *J. Nat. Prod.* **2007**, 70, 461–477.
- 20) Berdy, J. Proceedings of 9th International symposium on the biology of actinomycetes. **1995**. Allerton, New York, pp 3-23.
- 21) Hawksworth, D. L.; Rossman, A. Y. *Phytopathology* **1997**, 87, 888–891.
- 22) Soule, H. D.; Vazquez, J.; Long, A.; Albert, S.; Brennan, M. *J. Natl. Cancer Inst.* **1973**, 51, 1409–1416.
- 23) Carney, D. N.; Gazdar, A. F.; Bunn, P. A., Jr.; Guccion, J. G. *Stem Cells* **1982**, 1, 149–164.
- 24) Rosenblum, M. L.; Gerosa, M. A.; Wilson, C. B.; Barger, G. R.; Pertuiset, B. F.; de Tribolet, N.; Dougherty, D. V. *J. Neurosurg.* **1983**, 58, 170–176.
- 25) Bennett, G.J., Lee, H.H., *Phytochemistry*. **1989**, 28, 967.
- 26) Nakatani, K.; Nakahata, N.; Arakawa, T.; Yasuda, H.; Ohizumi, Y. *Biochem. Pharmacol.*, **2002**, 63, 73.
- 27) Suksamrarn, S.; Suwannapoch, N.; Phakhodee, W.; Thanuhiranlert, J.; Ratananukul, P.; Chimnoi, N.; Suksamrarn, A. *Chem. Pharm. Bull.*, **2003**, 51, 857.
- 28) Rath, G.; Potterat, O.; Mavi, S.; Hostettmann, K. *Phytochemistry*, **1996**, 43, 513.
- 29) Mahabusarakam, W.; Proudfoot, J.; Taylor, W.; Croft, K. *Free Radic. Res.*, **2000**, 33, 643.
- 30) Heald RA, Dexheimer TS, Vankayalapati H, Siddiqui-Jain A, Szabo LZ, Gleason-Guzman MC, Hurley LH. *J Med Chem* **2005**. 48:2993–3004
- 31) Shen, R, Wang, P, Tang, N. *J. Fluoresc.* **2010**, 20: 1287-1297.
- 32) Alali, F. Q.; El-Elimat, T.; Li, C.; Qandil, A.; Alkofahi, A.; Tawaha, K.; Burgess, J. P.; Nakanishi, Y.; Kroll, D. J.; Navarro, H. A.; Falkinham, J. O., III; Wani, M. C.; Oberlies, N. H. *J. Nat. Prod.* **2005**, 68, 173–178.